JBC RESEARCH ARTICLE

Grp78 destabilization of infectious prions is strain-specific and modified by multiple factors including accessory chaperones and pH

Received for publication, December 18, 2023, and in revised form, April 1, 2024 Published, Papers in Press, May 6, 2024,
https://doi.org/10.1016/j.jbc.2024.107346

Daniel Shoup* and **Suzette A. Priola**

From the Rocky Mountain Laboratories, Laboratory of Neurological Infections and Immunity, National Institute of Allergy & Infectious Diseases, National Institutes of Health, Hamilton, Montana, USA

Reviewed by members of the JBC Editorial Board. Edited by Ursula Jakob

Lethal neurodegenerative prion diseases result from the continuous accumulation of infectious and variably protease-resistant prion protein aggregates (PrP^D) which are misfolded forms of the normally detergent soluble and protease-sensitive cellular prion protein. Molecular chaperones like Grp78 have been found to reduce the accumulation of PrP^D, but how different cellular environments and other chaperones influence the ability of Grp78 to modify PrP^D is poorly understood. In this work, we investigated how pH and protease-mediated structural changes in PrP^D from two mouse-adapted scrapie prion strains, 22L and 87V, influenced processing by Grp78 in the presence or absence of chaperones Hsp90, DnaJC1, and Stip1. We developed a cell-free *in vitro* system to monitor chaperone-mediated structural changes to, and disaggregation of, PrP^D. For both strains, Grp78 was most effective at structurally altering PrP^D at low pH, especially when additional chaperones were present. While Grp78, DnaJC1, Stip1, and Hsp90 were unable to disaggregate the majority of PrP^D from either strain, pretreatment of PrP^D with proteases increased disaggregation of 22L PrP^D compared to 87V, indicating strain-specific differences in aggregate structure were impacting chaperone activity. Hsp90 also induced structural changes in 87V PrP^D as indicated by an increase in the susceptibility of its n-terminus to proteases. Our data suggest that, while chaperones like Grp78, DnaJC1, Stip1, and Hsp90 disaggregate only a small fraction of PrP^D, they may still facilitate its clearance by altering aggregate structure and sensitizing PrP^D to proteases in a strain and pH-dependent manner.

Infectious prions are the causative agents of lethal and transmissible mammalian prion diseases (1), such as scrapie in sheep, bovine spongiform encephalopathy in cattle, chronic wasting disease in deer and elk, and Creutzfeldt-Jakob disease (CJD) in humans (1). The gradual onset of disease and neurodegeneration during prion infection is associated with the continuous accumulation of non-native, infectious, and variably protease-resistant aggregates of the disease-associated prion protein (PrP^D), which are formed by the conversion of the native and protease-sensitive mammalian prion protein (PrP^C) into PrP^D (2). During PrP^D formation, which occurs at or near the cell surface and throughout the endosomal trafficking network (3–6), PrP^C adopts the same conformation of the PrP^D that it interacts with (7). However, multiple non-native prion protein conformations produce the infectious and protease-resistant aggregates that are characteristic of PrP^D and help define unique prion strains (8–10). Prion strains can have distinctive neuropathologies (11, 12), structural stabilities (13), routes of cellular endocytosis (14), and cellular degradation rates (15, 16).

Cellular systems attempt to combat the accumulation of infectious prions by internalizing PrP^D and trafficking it through the endosome to the lysosome, which is believed to be the primary site of prion degradation (17, 18). In our previous work, cells were found to begin degrading PrP^D during uptake by first sensitizing it to proteases and then destabilizing the aggregate structure, resulting in the exposure of protease-sensitive material buried within larger aggregates to proteases (15, 19). Thus, while the cellular processes responsible for destabilizing PrP^D during endocytosis are poorly understood, acidification of vesicle environments during endosomal trafficking appears to play a role in both sensitization of PrP^D to proteases and its degradation (15, 18). PrP^C has been found to unfold when exposed to lower pH environments (20) and exposure to low pH during trafficking may also drive the structural destabilization of PrP^D observed during endosomal trafficking (15, 19). However, changes in pH may also promote the ability of endosomal proteins, like molecular chaperones, to alter the structural properties of PrP^D.

Chaperones play a critical role in protein homeostasis throughout the cell and can disassemble non-native protein aggregates (21), unfold non-native proteins (22), and facilitate the folding of proteins into their native conformation (23). Chaperones belonging to the Hsp70 protein family are ATP-driven protein conformation modifiers that contribute to almost every aspect of cellular proteostasis (24) and have been found to play a role in prion biology (25). In cells infected with the RML strain of PrP^D, the concentration of the membrane-bound Hsp70 protein Grp78, also known as BiP, is inversely proportional to the concentration of PrP^D (25). Grp78 typically

* For correspondence: Daniel Shoup, daniel.shoup@nih.gov.

localizes to the endoplasmic reticulum (ER) but is regularly translocated to the cell surface, where PrP^D may be found. This translocation is dependent upon its ATP hydrolysis stimulating protein recruitment co-chaperone DnaJC1 (26, 27). Previous studies have shown that the formation of *de novo* PrP^D can happen almost immediately following the interaction of PrP^D and PrP^C on the cell surface (28), but Grp78 takes almost 20 h to reduce the PK resistance of RML PrP^D by 50% at neutral pH in a cell-free *in vitro* assay (25), indicating that Grp78 alone is likely incapable of clearing PrP^D faster than it is created. However, Grp78 can escort protein cargo through the endosomal trafficking network to the late endosome (29) and remains active at pH 5.5 (30), which is the pH of vesicles in the late endosome (31). Thus, structural destabilization and modification of PrP^D during cellular uptake as a result of changes in endosomal pH and exposure to proteases could influence its structural destabilization by Grp78.

Other chaperones and co-chaperones may facilitate the activity of Grp78 and be required for the timely processing of PrP^D. For example, the Hsp90 chaperone and its substrate recruitment co-chaperone Stip1 (32), which have been observed interacting with and altering the structure of PrP^C on the surface of cells (33, 34), may also interact with PrP^D. Stip1 can also recruit Hsp70 chaperones to Hsp90, forming a multi-chaperone complex between Hsp70, Stip1, and Hsp90, that allows for substrate protein to pass from Hsp70 to Hsp90 (35). This multi-chaperone complex may promote the binding of Hsp90 to PrP^D in cases where differences in strain conformation (7, 36) or protease exposure (37) obscure or remove Stip1 binding sites on the n-terminus (38). Stip1 also promotes endocytosis of PrP^C through direct interaction (39), suggesting that co-complexed Hsp90 and Grp78 could accompany PrP^C, and possibly PrP^D, during endocytosis. Members of the Hsp90 chaperone family are active at low pH and undergo conformational changes with pH shifts that influence chaperone activity (40, 41). Hsp90 may thus facilitate changes in PrP^D alongside Grp78 even in the low pH environments of the late endosome. While previous observations make it appear possible that Hsp90 and Stip1 play a role in Grp78-mediated regulation of PrP^D, how chaperones co-ordinate to influence the properties of PrP^D and their role in PrP^D degradation are poorly understood.

We therefore characterized how changes in pH, protease exposure, and the presence of the chaperones Hsp90, Stip1, and DnaJC1 influence the ability of Grp78 to alter the size and structure of PrP^D from two unique prion strains, 22L and 87V. Our data show that at a lower pH, PrP^D from both strains is conformationally altered by Grp78 within 30 min, becoming less stable and thus more sensitive to loss of protease protection. The addition of auxiliary chaperones enhanced the ability of Grp78 to sensitize both strains to proteases in high- and low-pH solutions, but 22L PrP^D was consistently more susceptible to structural destabilization by chaperones than 87V. While 22L PrP^D pre-treated with proteases was the most susceptible to disaggregation, the majority of PrP^D was not disaggregated for either strain, regardless of experimental condition or observation of structural change. Taken together, our data suggest that pH, Grp78, and auxiliary chaperones can work synergistically to destabilize the structure of PrP^D. This may facilitate the degradation of PrP^D as it is trafficked further along the endolysosomal pathway and through multiple cycles of exposure to proteases, chaperones, and shifts in pH. These data not only highlight the importance of chaperones in the processing and clearance of PrP^D but also suggest the chaperones that could be involved and the subcellular localizations where they could contribute to the effective processing of prion aggregates.

Results

Exposure to Grp78 and low pH reduces PrP^D protease-resistance in a strain-specific manner

We first asked how pH influences the ability of Grp78 to alter the structural properties of PrP^D from different prion strains by determining how the PK resistance of PTA precipitated 22L and 87V PrP^D changed with incubation in different pH-buffered solutions. PTA precipitated total PrP^D from both strains was incubated for 30 min in solutions with pH values ranging from 7.4 to 5.5, which respectively correlate with the physiological pH values recorded on the surface of cells (42) and in the late endosome (43), before being treated with PK and then de-glycosylated with PNGase F. Samples were then analyzed *via* Western blot using the 6D11 anti-PrP antibody, and the PK resistance of both 22L and 87V PrP^D at each pH was calculated. Following de-glycosylation, full-length and n-terminally truncated PrP^D can be seen at molecular weights of approximately 25 and 20 kDa, respectively (Fig. 1*A*). While the PK resistance of both 22L and 87V PrP^D decreased with pH, the PK resistance of 22L PrP^D was significantly lower than that of 87V PrP^D at pH 5.5, with the PK resistance of 22L and 87V populations decreasing by ∼80% and ∼55%, respectively, from pH 7.4 to 5.5. Changes in PK resistance are often used to measure the conformational and structural stability of PrP^D strains (44, 45), as loss of a protein's properties can result from changes in the conformation of the protein and/or the structure of the oligomers they form. Thus, the greater loss of PK resistance in populations of 22L PrP^D at low pH when compared to populations of 87V PrP^D suggests that the structure of 22L PrP^D is less pH stable than that of 87V. This is consistent with previous observations that 22L PrP^D is generally less stable than 87V (16, 19).

Total PrP^D from both 22L and 87V was less stable at a pH of 5.5, which could facilitate further structural destabilization by molecular chaperones. To test this, we employed an *in vitro* cell-free chaperone system. Total PrP^D from both 22L and 87V was diluted into either a pH 7.4 or 5.5 buffer containing an ATP regenerating system (ATP, creatine phosphate, creatine kinase) before being incubated for 30 min with and without Grp78. Half of each sample was used to test the protease-resistance of PrP^D as well as the protection of the protease-sensitive PrP^D n-terminus of full-length PrP^D (Fig. 1, *B–D*), which was previously determined to be a good marker for destabilization of aggregate structure (19). The other half of

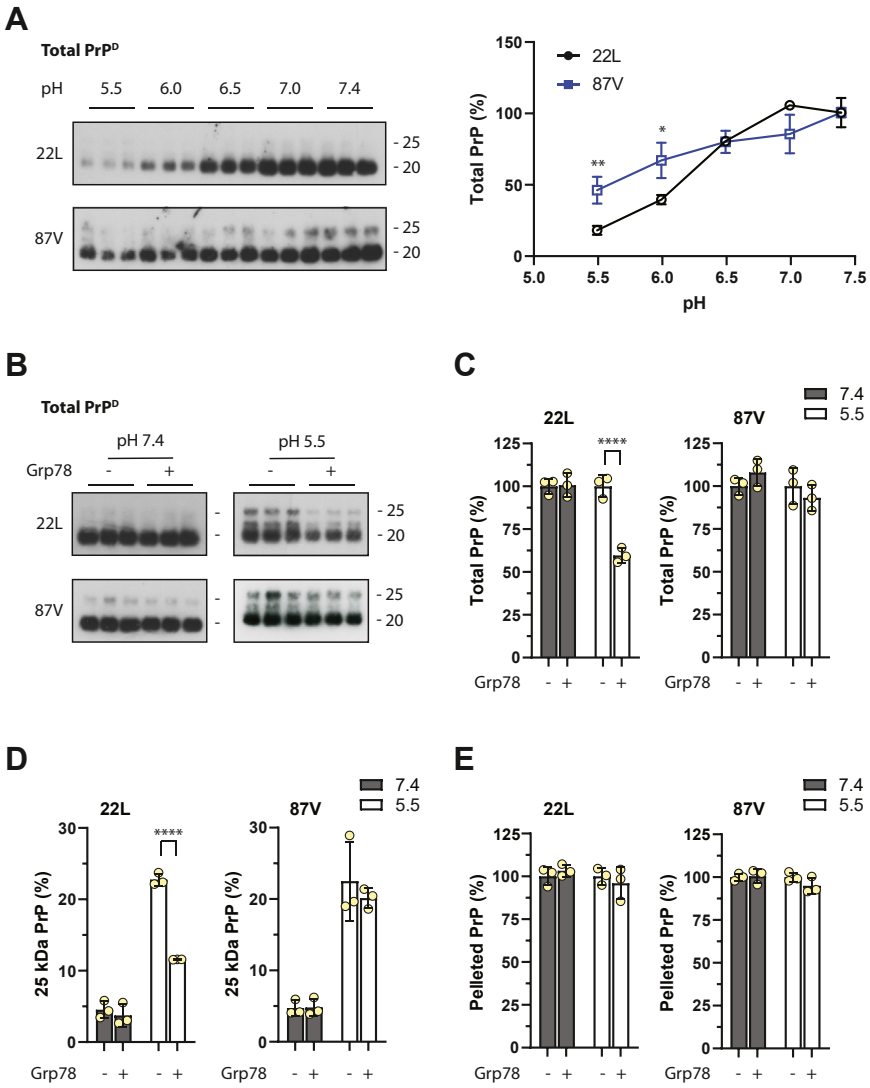

Figure 1. Grp78 mediates a prion strain and pH-dependent change in PrP^D structure in the absence of disaggregation. *A*, Western blot of total PrP^D from 22L (*upper left panel*) and 87V (*lower left panel*) that was PTA precipitated from brain homogenate of prion-infected mice and incubated at the indicated pH for 30 min before being PK treated. The percentage of PrP^D remaining at each pH was plotted as shown in the *right panel* for 22L (*black line* and *open circles*) and 87V (*blue line open squares*). Significance was determined using a two-way ANOVA Tukey multiple comparisons test. $p^* = 0.013$; $p^{**} = 0.009$. *B*, Western blot of PTA precipitated total PrP^D from 22L (*upper panel*) and 87V (*lower panel*) that was incubated for 30 min at a pH of 7.4 or 5.5 with (+) or without (–) Grp78 and then treated with PK. All samples contained both ATP and an ATP regeneration system. PrP^D remaining after PK treatment was quantified (*C*) and the percentage of total PrP^D was calculated by dividing the amount of 22L (*left panel*) and 87V (*right panel*) PrP^D present at pH 7.4 or pH 5.5 by the average amount of PrP^D not exposed to Grp78. *D*, the percentage of 25 kDa, full-length, PrP^D protected from proteases at a pH of 7.4 or 5.5 for 22L (*left panel*) and 87V (*right panel*) for PrP^D that was (+) or was not (–) treated with Grp78. *E*, quantification of the amount of insoluble 22L (*left panel*) and 87V (*right panel*) PrP^D with (+) or without (–) previous exposure to Grp78. For all Western blots, samples were de-glycosylated by treatment with PNGase F before being analyzed and developed with the anti-PrP antibody 6D11. Size markers to the right of each immunoblot correlate to 25 kDa (*upper marker*) and 20 kDa (*lower marker*). For all graphs, data were calculated from n = 3 for each timepoint and are given as mean ± standard deviation. *Yellow circles* indicate individual data points. Significance was determined using an unpaired one-tail *t* test. $^{****}p = <0.0009$. For all bar graphs, *black bars* = pH 7.4; *white bars* = pH 5.5.

each sample was used to test for PrP^D disaggregation *via* sedimentation assay (Fig. 1*E*). Samples treated with Grp78 were then normalized to samples not treated with Grp78 to facilitate comparison between strains and experiments. At a pH of 7.4, neither 22L nor 87V PrP^D exhibited increased PK sensitivity in the presence of Grp78 (Fig. 1, *B* and *C*). However, at a pH of 5.5, Grp78 further sensitized about half of the total amount of PrP^D from 22L, but not 87V, to PK with increased exposure of the n-termini of full-length, 25 kDa, PrP^D (Fig. 1, *B–D*) but no noticeable disaggregation (Fig. 1*E*). Interestingly, full-length PrP^D in both 22L and 87V populations was better protected from PK at a pH of 5.5 than at 7.4, indicating that a subpopulation of protease-resistant PrP^D is undergoing a pH-dependent change in structure that results in better protection of its protease-sensitive n-termini (Fig. 1, *B–D*). Additionally, a 23 kDa truncation product was observed in both 22L and 87V at a pH of 5.5 (Fig. 1*B*), further supporting the possibility that a subpopulation of PrP^D is only partially accessible to proteases at pH 5.5. While the n-terminus of PrP^D is sensitive to proteolytic degradation, previous work has found that full-length

PrP^D can be fully or partly protected from proteases within larger aggregates (19), which may explain the presence of the 23 kDa band. Taken together, these data indicate that acidification-induced destabilization of PrP^D appears to facilitate aggregate structural destabilization by Grp78 in a strain-dependent manner.

Co-chaperones DnaJC1 and Stip1 promote Grp78-mediated structural changes in 22L and 87V PrP^D at low pH

Modulation of the Grp78 binding cycle by ATPase stimulating co-chaperones DnaJC1 (27) and Stip1 (46, 47) could facilitate Grp78-mediated structural change in PrP^D, allowing Grp78 to more effectively sensitize PrP^D to proteases. Additionally, the presence of DnaJC1 may also help by directly recruiting PrP^D to Grp78. To determine if these co-chaperones could influence the ability of Grp78 to destabilize PrP^D, total PrP^D from 22L and 87V was mixed with an ATP regeneration system containing DnaJC1 or Stip1 at a pH of either 7.4 or 5.5. Half of each sample set was then incubated with Grp78 for 30 min before being tested for changes in PK resistance by Western blot (Fig. 2*A*). At a pH of 7.4, the presence of DnaJC1 or Stip1 did not change the sensitivity of 22L or 87V PrP^D to proteases in the presence of Grp78 (Fig. 2, *A* and *B*). However, for both strains, the ability of Grp78 to sensitize total PrP^D to PK was enhanced by the presence of either DnaJC1 or Stip1 at a pH of 5.5. Compared to samples not treated with Grp78, 22L lost almost 75% of its resistance to PK (Fig. 2, *A* and *B*), 25% more than observed with Grp78 alone (Fig. 1, *B* and *C*). Even more significant, 87V PrP^D lost nearly 50% of its resistance to PK in the presence of Grp78 and either co-chaperone (Fig. 2, *A* and *B*), while Grp78 alone

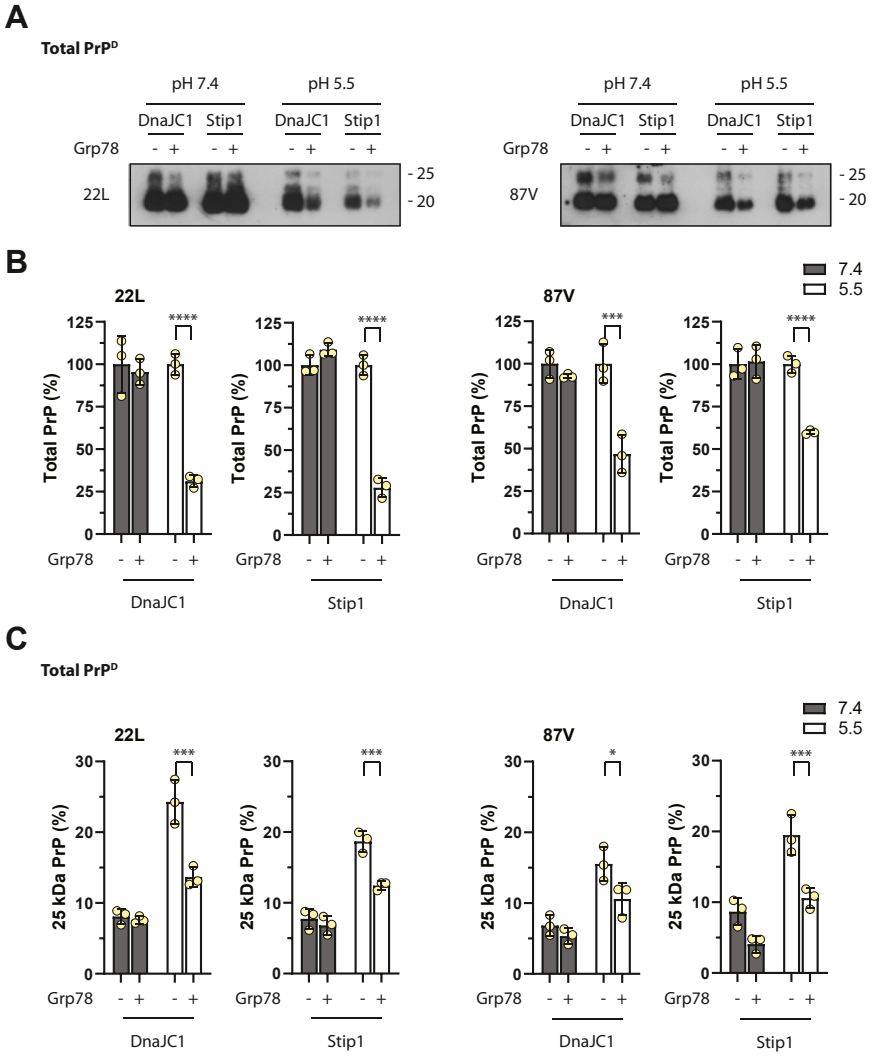

Figure 2. The co-chaperones DnaJC1 and Stip1 promote Grp78-mediated modification of 22L and 87V PrP^D. *A*, representative Western blots of 22L (*left panel*) and 87V (*right panel*) total PrP^D incubated with DnaJC1 or Stip1 in the presence (+) or absence (–) of Grp78. The 25 kDa (*upper marker*) and 20 kDa (*lower marker*) size markers to the *right* of each immunoblot correlate with 25 kDa, full-length, and n-terminally truncated PrP^D, respectively. All samples were treated with PK followed by treatment with PNGase F. The immunoblots were developed with the anti-PrP 6D11 mouse monoclonal antibody. *B*, immunoblots were quantified, and the percentage of 22L (*left plots*) and 87V (*right plots*) PrP^D remaining after PK treatment was determined. *C*, the percentage of 25 kDa, full-length, PrP^D remaining after PK treatment for 22L (*left plots*) and 87V (*right plots*). For all graphs, *black bars* = pH 7.4; *white bars* = pH 5.5. All data were calculated from n = 3 for each group and are given as mean ± standard deviation. An unpaired one-tail *t* test was used to calculate the statistical significance between data. *Asterisks* represent a range of *p*-values with $p^* = 0.03$, $p^{***} = 0.001$ to 0.004, and $p^{****} = <0.0009$.

had no effect at the same pH (Fig. 1, *B* and *C*). Thus, the addition of either co-chaperone stimulated a similar degree of PK sensitization for PrP^D from each strain. While the co-chaperones did not appear to facilitate the Grp78-mediated sensitization of the n-terminus of 22L PrP^D to proteases (compare Fig. 1*D* to Fig. 2*C*), the presence of either co-chaperone facilitated the ability of Grp78 to expose the n-terminus of 87V PrP^D to PK at pH 5.5 (Fig. 2*C*, right panels). Taken together, the data show that the presence of DnaJC1 or Stip1 stimulated the ability of Grp78 to sensitize total PrP^D to proteases. In addition, loss of PK resistance in both 22L and 87V PrP^D at acidic pH suggests that pH-dependent structural destabilization also facilitates the activity of Grp78 against both strains, albeit in a strain-specific manner.

Proteolytic digestion alters the sensitivity of 22L and 87V PrP^D to structural destabilization by acidification and chaperone activity

Previous studies have shown that cellular processes are able to sensitize a portion of 22L and 87V PrP^D aggregates to proteases during cellular uptake, ultimately leading to the accumulation of a population of small, stable, protease-resistant PrP^D aggregates (15). Similarly, the present work shows that a combination of acidification and chaperone-induced structural change over 30 min was only able to partially sensitize 22L and 87V PrP^D to proteolytic degradation, indicating that the PrP^D aggregate core is highly stable and recalcitrant to structural destabilization. In order to determine how sensitive the protease-resistant core of PrP^D is to structural destabilization by changes in pH, 22L and 87V PrP^D were treated with PK prior to PTA precipitation to yield the highly protease-resistant PrP^D core, which was then incubated for 30 min at pH 7.4, 7.0, 6.5, 6.0, or 5.5 before being again treated with PK (Fig. 3*A*). Unlike total PrP^D that was not treated with PK prior to PTA, the protease-resistant cores of PrP^D from 22L and 87V PrP^D did not exhibit a significant decrease in protease-resistance as a result of the transition from pH 7.4 to 5.5 (compare Fig. 3*A* to Fig. 1*A*) Thus, the protease-resistant core of PrP^D that survives PK digestion is indeed less sensitive to pH-induced structural destabilization than total PrP^D.

We next sought to ascertain how sensitive the protease-resistant cores of 22L and 87V PrP^D were to chaperone-mediated structural destabilization. PK pre-treated PrP^D was incubated in an ATP regeneration system in pH 7.4 and 5.5 buffer with and without Grp78 (Fig. 3, *B* and *C*). Similarly to the total PrP^D samples, Grp78 was not able to sensitize the protease-resistant core of 87V to further protease digestion at either pH. As with total PrP^D, Grp78 was able to increase the protease-sensitivity of the protease-resistant core of 22L PrP^D at a pH of 5.5 though only to about 40% (compare Fig. 3, *B* and *C* to Fig. 1, *B* and *C*). However, it was also able to reduce the PK resistance of the protease-resistant core of 22L PrP^D at a pH of 7.4 by ~25%. This was not observed in the 22L total PrP^D samples at pH 7.4, where Grp78 had no effect (Fig. 1, *B* and *C*). Further examination of the protease-resistant core of 22L and 87V PrP^D showed that the amount of protease-protected n-termini in both strains remained the same following incubation with Grp78 at either pH (Fig. 3*D*), and no disaggregation was observed (Fig. 3*E*). The addition of DnaJC1 or Stip1 to the reaction at pH 5.5 marginally improved the ability of Grp78 to sensitize the protease-resistant core of 22L PrP^D to PK (compare Fig. 4*B* to Fig. 3*C*). There was no enhanced effect compared to Grp78 alone at a pH of 7.4 and no enhanced effect on the 87V PrP^D protease-resistant core at either pH (compare Fig. 4*B* to Fig. 3*C*). However, in the presence of either co-chaperone at any pH, Grp78 had a small but significant impact on increasing the sensitivity of the n-terminus of 87V, but not 22L, PrP^D to proteases (Fig. 4*C*). With the exception of 22L at a pH of 7.4, the protease-resistant core of PrP^D was less susceptible to alteration by Grp78, DnaJC1, and Stip1 when compared to total PrP^D (see Fig. 2), indicating that it is generally less sensitive to structural destabilization by pH and chaperones.

DnaJC1 and Stip1 facilitate Grp78-mediated disaggregation of the protease-resistant core of 22L PrP^D

Disaggregation of 22L and 87V PrP^D was not observed with Grp78 alone (Fig. 1*E*). However, since Grp78 was more capable of sensitizing PrP^D to PK in the presence of co-chaperones (Fig. 2), we considered that DnaJC1 and Stip1 could similarly promote disaggregation of total PrP^D and its protease-resistant core by Grp78. To determine the amount of 22L and 87V PrP^D solubilized by Grp78 in the presence of DnaJC1 or Stip1, we pelleted PrP^D after 30 min of exposure to chaperones and then compared the amount of PrP^D in the pellet and supernatant *via* immunoblot (Fig. S1). Regardless of the pH, strain, or combination of Grp78 and co-chaperone, the majority of PrP^D pelleted, indicating that Grp78 in the presence of either DnaJC1 or Stip1 was not solubilizing a significant proportion of PrP^D into small oligomers or monomers. However, longer exposures of immunoblots containing only the supernatant samples showed that some solubilization of the protease-resistant core of 22L, but not 87V, PrP^D occurred when incubated with Grp78 and its co-chaperones, with more material being solubilized at a pH of 5.5 than 7.4 (Fig. 5*A*). While the presence of Grp78 increased the amount of soluble PrP^D in the presence of either co-chaperone, a small amount of soluble prion protein was also observed in samples containing only DnaJC1 at both pH values (Fig. 5*B*). Hsp40 co-chaperones, like DnaJC1, are not known to perform disaggregation but have been observed preventing protein aggregation (48), suggesting that PK pre-treatment creates smaller aggregates of 22L that DnaJC1 may be preventing from re-aggregating. Overall the data are consistent with chaperones solubilizing a small amount of aggregated, highly protease-resistant PrP^D in a strain-specific manner.

Hsp90 facilitates protease-sensitization and disaggregation of PrP^D by Grp78 in a manner dependent upon strain, pH, and protease exposure

In order to ascertain the ability of Hsp90 to modify the structure of PrP^D, the relative protease-resistance of 22L and

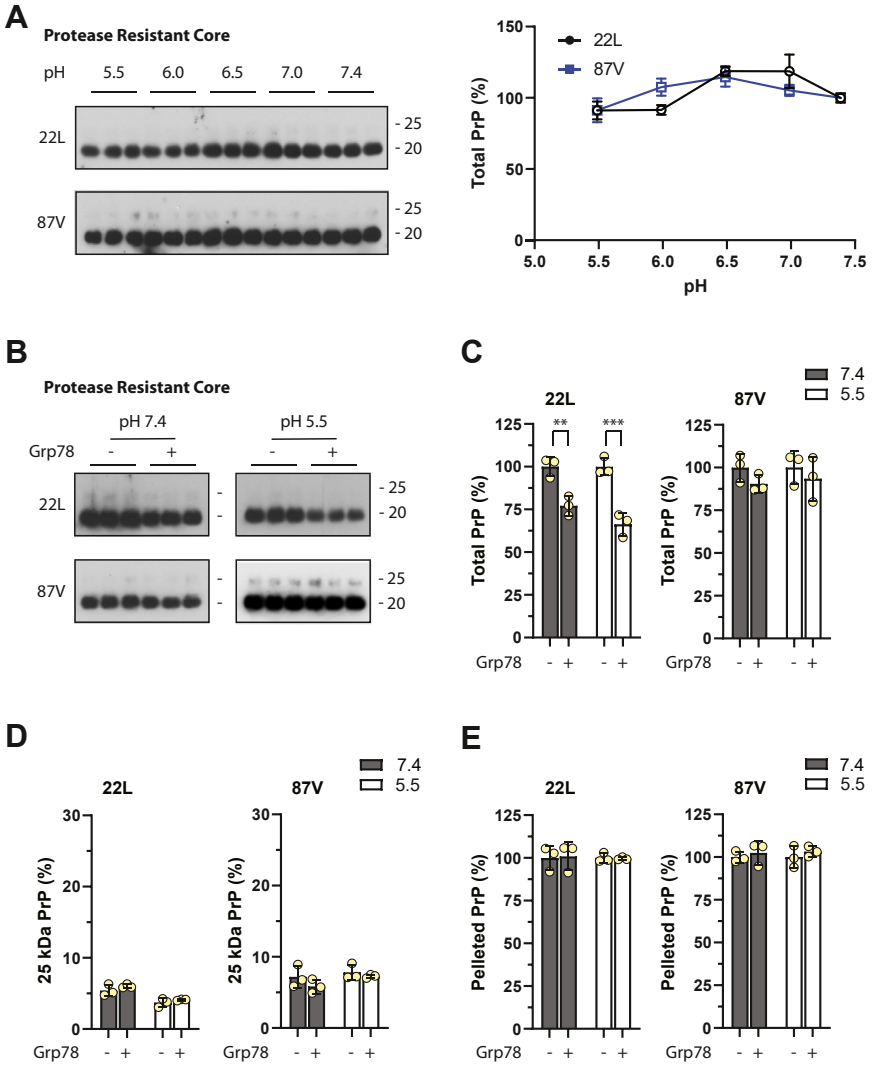

Figure 3. The protease-resistant core of PrP^D is less sensitive to destabilization by pH and Grp78. *A*, Western blot of the PK treated, PTA precipitated protease-resistant core of PrP^D from 22L (*upper left panel*) and 87V (*lower left panel*) incubated at different pH prior to a second PK digestion. The percentage of PrP^D remaining was calculated and is plotted as shown in the *right panel* for 22L (*black line* and *open circles*) and 87V (*blue line open squares*). *B*, the protease-resistant core of 22L PrP^D (*upper panels*) and 87V PrP^D (*lower panels*) was incubated for 30 min at a pH of 7.4 (*left panels*) or 5.5 (*right panels*) with (+) or without (–) Grp78 before being digested with PK and analyzed *via* immunoblot. All samples contained ATP and an ATP regeneration system. *C*, the percentage of PrP^D remaining at pH 7.4 or 5.5 was calculated for 22L (*left plot*) and 87V (*right plot*). *D*, the percentage of 25 kDa, full-length, PrP^D protected from proteases for the samples in panel *B*. Shown are 22L (*left panel*) and 87V (*right panel*) at a pH of 7.4 or 5.5 that was (+) or was not (–) treated with Grp78. *E*, the amount of insoluble 22L (*left plot*) and 87V (*right plot*) protease-resistant PrP^D that pelleted out of solution with (+) and without (–) previous exposure to Grp78. All samples were de-glycosylated by treatment with PNGase F before being analyzed by immunoblot and developed with the anti-PrP mouse monoclonal antibody 6D11. Size markers to the right of each immunoblot correlate to 25 kDa (*upper marker*) and 20 kDa (*lower marker*). For all graphs, data were calculated from n = 3 for each timepoint and are given as mean ± standard deviation. An unpaired one-tail *t* test was used to calculate the statistical significance shown in panel *C*. $p^{**} = 0.007$ and $p^{***} = 0.002$. *Black bars* = pH 7.4; *white bars* = pH 5.5.

87V PrP^D was characterized after exposure to either Grp78, Hsp90, or a combination of both chaperones. Both DnaJC1 and Stip1 were present in all samples and assays were performed at a pH of 7.4 and 5.5 against either total PrP^D (Fig. 6) or the PrP^D protease-resistant core (Fig. 7). In samples of total PrP^D, Hsp90 alone was not able to significantly reduce the PK resistance of 22L, while the combination of both Hsp90 and Grp78 reduced the PK resistance of 22L by nearly 50% and 90% at a pH of 7.4 and 5.5, respectively (Fig. 6*A*). By contrast, Hsp90 had no impact on the PK resistance of 87V PrP^D alone and Hsp90 did not enhance the activity of Grp78 on 87V (Fig. 6*A*). However, in combination with Grp78 at pH 7.4, it did significantly increase the exposure of the n-terminus of total PrP^D from 87V to proteolytic digestion (Fig. 6*B*).

When incubated with the protease-resistant core of either 22L or 87V PrP^D, Hsp90 alone did not significantly reduce its protease-resistance (Fig. 7*A*), although there was again an increased exposure of the n-terminus of 87V PrP^D to proteolytic degradation at pH 7.4 (Fig. 7*B*). Furthermore, at pH 5.5, the susceptibility of the n-terminus of 87V PrP^D to PK was increased by exposure to the full set of chaperones (Fig. 7*B*), such that no trace of full-length 25 kDa PrP^D could be detected even following over-exposure of the immunoblots (Fig. S2). Thus, while Hsp90 did little to reduce the PK resistance of 22L

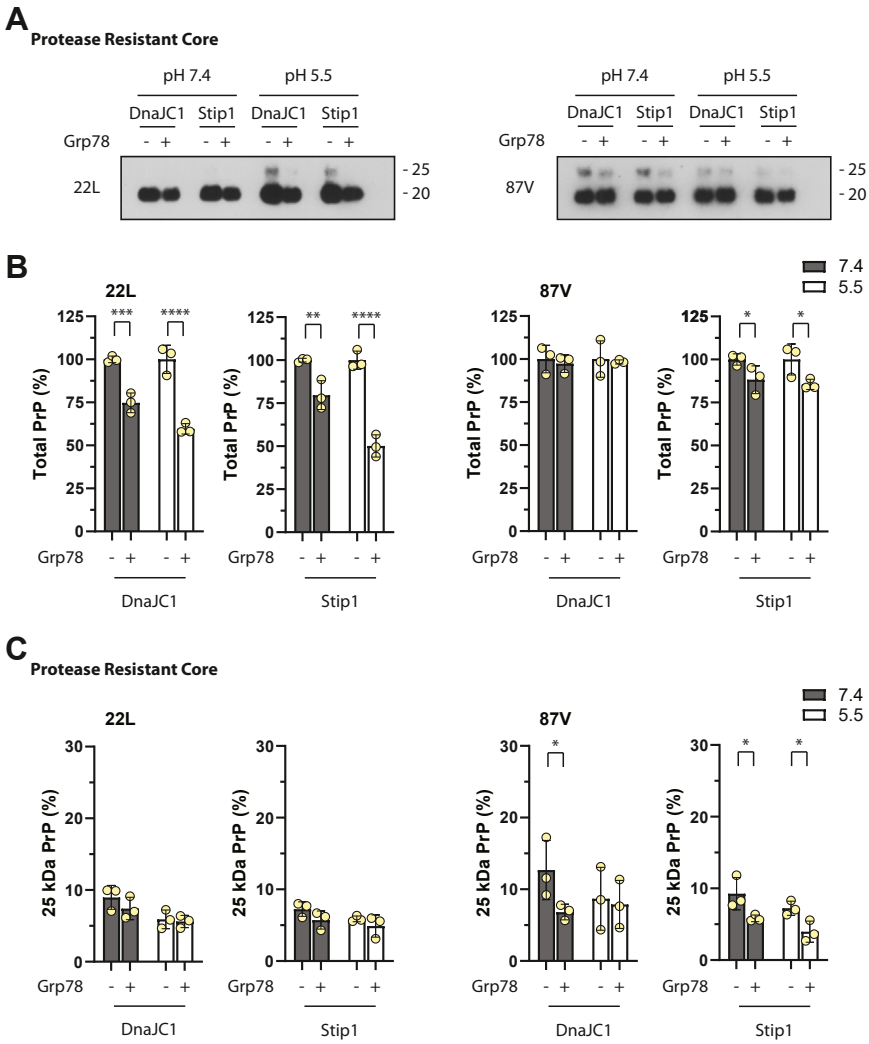

Figure 4. Protease treatment alters the susceptibility of 22L and 87V PrP^D to Grp78 in the presence of co-chaperones DnaJC1 or Stip1. *A*, Western blot of the protease-resistant core of 22L (*left panel*) and 87V (*right panel*) PrP^D mixed with DnaJC1 or Stip1 at pH 7.4 or 5.5 before being incubated for 30 min with (+) or without (–) Grp78 and an ATP regeneration system. Samples were then treated with PK before being de-glycosylated with PNGase F and analyzed *via* Western blot using the 6D11 antibody. Size markers to the right of blots indicate 25 kDa (*upper marker*) and 20 kDa (*lower marker*). *B*, quantification of the amount of the protease-resistant core of 22L (*left plots*) and 87V (*right plots*) PrP^D remaining following exposure to chaperones at pH 7.4 or pH 5.5. *C*, for the protease-resistant core of PrP^D following exposure to chaperones at pH 7.4 or pH 5.5, the percentage of 25 kDa, full-length, 22L (*left plots*) and 87V (*right plots*) PrP^D that survived PK treatment was quantified. For all graphs, data were calculated from n = 3 for each condition and are given as mean ± standard deviation. An unpaired one-tail *t* test was used to calculate the statistical significance. *Asterisks* represent a range of *p*-values with p^* = 0.01 to 0.04, p^{**} = 0.007, p^{***} = 0.001, and p^{****} = <0.0009. *Black bars* = pH 7.4; *white bars* = pH 5.5.

and 87V PrP^D on its own, in the presence of Grp78 it enabled further reduction of the PK resistance of 22L PrP^D and further exposure of the n-terminus of 87V PrP^D. Overall, the data suggest that Hsp90's ability to alter PrP^D is strain-specific and that it either works synergistically with Grp78 to unfold PrP^D or requires Grp78 for recruitment to PrP^D.

The combined activity of Hsp90, Grp78, DnaJC1, and Stip1 at pH 5.5 reduces the protease-resistance of 22L by nearly 90% (see Fig. 6), but also greatly exposes the n-terminus of 87V to proteases (see Fig. 7), suggesting that these chaperones may be destabilizing PrP^D around its n-terminus. It is thus possible that these chaperones are destabilizing the region of PrP from amino acids 93 to 109, the location of the epitope for the 6D11 anti-PrP antibody used throughout this work, allowing PK to access this region. This could lead to loss of the region of PrP^D containing just the 6D11 epitope, with the rest of PrP^D remaining protease-resistant. In order to determine the amount of total PrP^D that completely loses resistance to PK as opposed to only losing the 6D11 epitope, total PrP^D from 22L and 87V was exposed to Hsp90, Grp78, DnaJC1, and Stip1 at pH 7.4 and 5.5 before being analyzed *via* immunoblot with the Saf84 antibody (Fig. 8). Saf84 recognizes a more c-terminal region of PrP^D from amino acids 159 to 169. In the absence of chaperones, the banding patterns of 22L and 87V observed with the Saf84 antibody were similar to those observed with the 6D11 antibody (compare Fig. 8*A* to Fig. 6*A*). However, when immunoblots were developed with the Saf84 antibody, a lower molecular weight band of about 16-17 kDa consistent with loss of the PrP^D n-terminus was observed at both pH 5.5 and 7.4 in samples of 22L total PrP^D exposed to the full set of chaperones (Fig. 8*A*). When 22L exposed to all chaperones at pH 5.5 was further probed with the 31C6 (a.a. 143-149) and mab 132 (a.a.

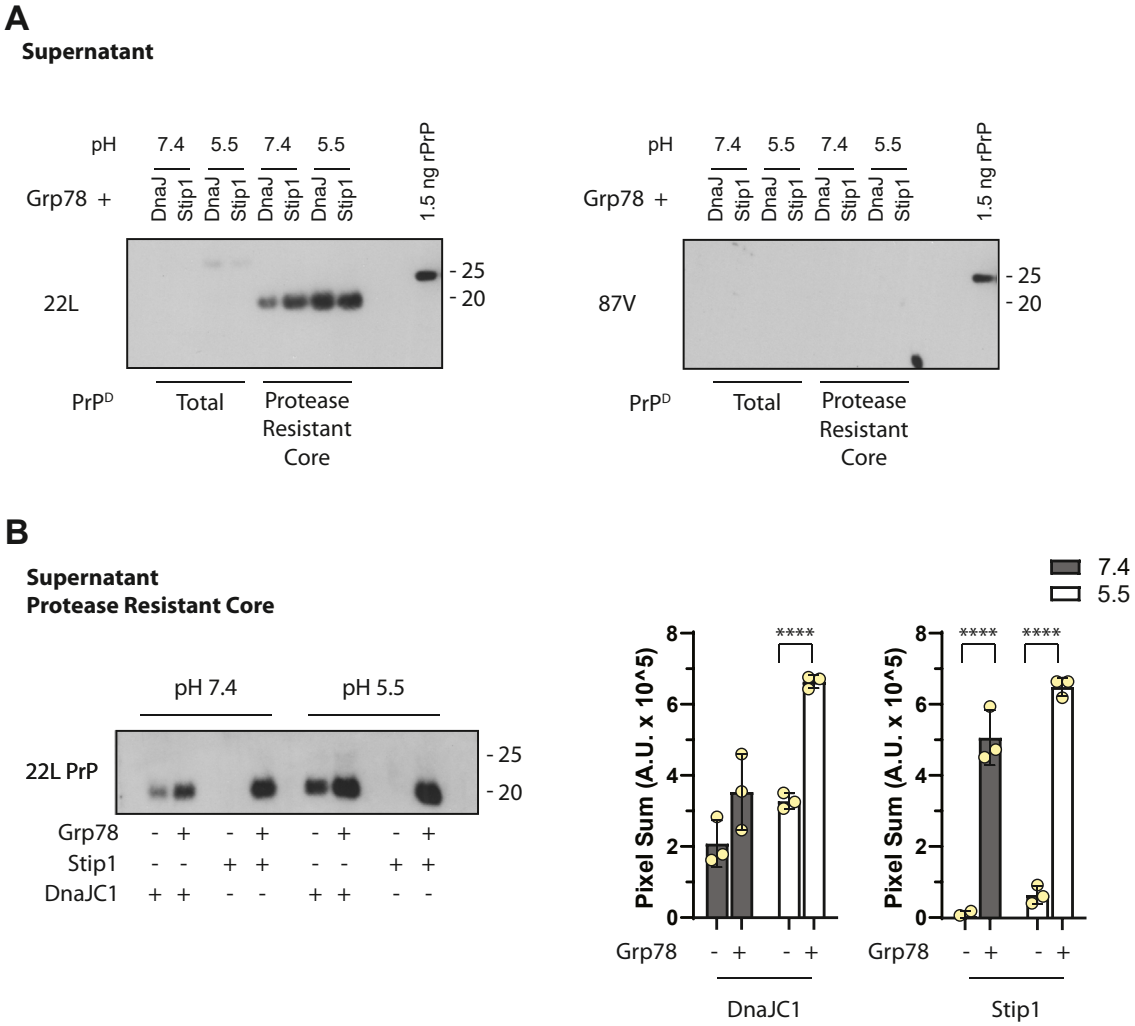

Figure 5. The co-chaperones DnaJC1 and Stip1 promote Grp78-mediated disaggregation of the protease-resistant core of 22L PrP^D. The relative amounts of total PrP^D and its protease-resistant core disaggregated by combinations of Grp78, DnaJC1, or Stip1 at pH 7.4 and 5.5 were determined *via* immunoblot. *A*, representative long exposure immunoblots, using the same supernatant samples shown in Fig. S1, of the supernatants from centrifuged total PrP^D or its protease-resistant core from 22L (*left panel*) and 87V (*right panel*) following incubation with combinations of Grp78, DnaJC1, or Stip1, at pH 7.4 and 5.5. Recombinant PrP (1.5 ng, rPrP) was used to control for exposure times between both blots. *B*, representative immunoblots (*left panel*) and quantitation (*right panel*) of the amount of the protease-resistant core of 22L PrP^D that was solubilized following exposure to different combinations of Grp78, DnaJC1, and Stip1 at pH 7.4 or 5.5. All samples were PNGase F treated before being analyzed by Western blot. Molecular weight markers for 25 kDa (*upper marker*) and 20 kDa (*lower marker*) are shown to the *right* of each blot. The amount of solubilized PrP^D was quantified and is shown as a sum of pixels in arbitrary units. Data shown were calculated from n = 3 for each sample and are given as mean ± standard deviation. An unpaired one-tail *t* test was used to calculate the statistical significance. ****p value $<$ 0.0009. *Black bars* = pH 7.4, *white bars* = pH 5.5.

119-127) antibodies (49), the lower molecular weight band was detected by 31C6 but not mab 132, indicating that it was a c-terminal fragment of PrP^D approximately 16 kDa in size (Fig. S3). This band was not observed in samples of 87V total PrP^D (Fig. 8, *A* and *B*) or on immunoblots developed with the 6D11 antibody (Fig. 7), indicating that the ∼16 kDa band lacks the 6D11 epitope. Thus, the chaperone mediated loss of protease resistance in 22L PrP^D is the result of partial loss of protease resistance through n-terminal residues 119-127.

The total amount of the ∼16 kDa band was ∼20 and ∼55% of the 22L PrP^D population at pH 7.4 and 5.5 respectively (Fig. 8*B*), indicating that the amount of 22L that completely lost resistance to PK in the presence of all chaperones set was ∼43% at pH 7.4 and ∼38% at pH 5.5. By contrast, loss of protease-resistance in 87V was due to either loss of the n-terminus of PrP^D up to amino acid residue 169 or the complete sensitization of PrP^D to proteases. The 16 kDa band produced by the interaction of chaperones with PrP^D is similar to a c-terminal fragment that has been observed following partial chemical denaturation and subsequent protease digestion of PrP^D (50). This is consistent with the 16 kDa c-terminal fragment of PrP^D being a highly protease-resistant species of PrP^D that is the result of structural destabilization (50). These data demonstrate not only that chaperones can sensitize a significant portion of the PrP^D n-terminus to proteases in a prion strain-specific manner, but also suggest how they may contribute to the disaggregation and/or degradation of prions within the cell.

The combined activity of Hsp90, Grp78, DnaJC1, and Stip1 greatly reduced the PK resistance of 22L PrP^D. We

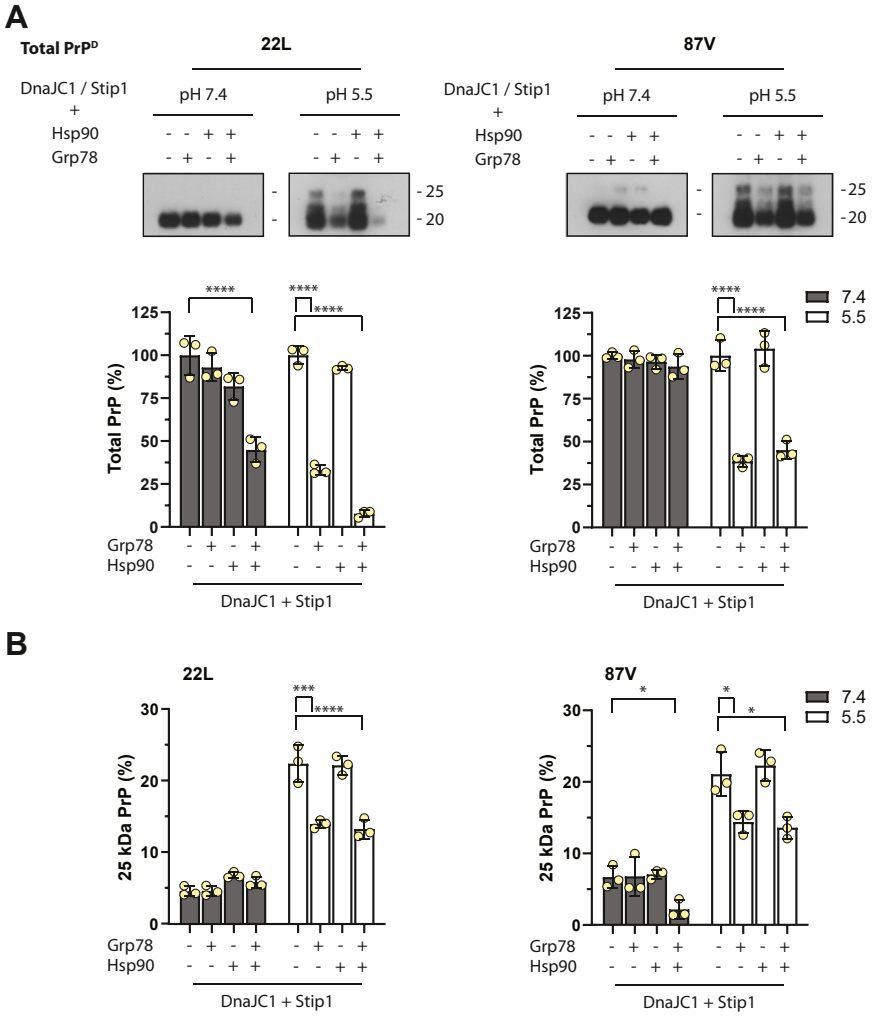

Figure 6. Hsp90 can cooperate with Grp78 to enhance the sensitivity of total PrP^D to proteases. *A*, representative Western blots of total PrP^D from 22L (*upper left panels*) or 87V (*upper right panels*). PrP^D was mixed with DnaJC1 and Stip1 at a pH of 7.4 or 5.5 before being incubated with either Grp78, Hsp90, or Grp78/Hsp90, for 30 min in the presence of an ATP regeneration system. Samples were then treated with PK and de-glycosylated with PNGase F before being run over a gel and analyzed by Western blot with the 6D11 anti-PrP monoclonal antibody. To the *right* of each blot are 25 kDa (*upper marker*) and 20 kDa (*lower marker*) size markers. *Lower panels* show the percentage of total PrP^D from 22L (*lower left plot*) or 87V (*lower right plot*) remaining following exposure to chaperones and PK. *B*, percentage of 25 kDa, full-length, PrP^D remaining after exposure to chaperones and PK treatment for 22L (*left plot*) and 87V (*right plot*). For all bar plots, data were calculated from n = 3 for each sample and are given as mean ± standard deviation. A one-way ANOVA with Tukey multiple comparisons within each pH data set was used to calculate the statistical significance. *Asterisks* represent a range of *p*-values with p^* = 0.01 to 0.04, p^{***} = 0.001, and p^{****} = <0.0009. *Black bars* = pH 7.4; *white bars* = pH 5.5.

hypothesized that the presence of Hsp90 could also be facilitating Grp78-mediated disaggregation of 22L and 87V PrP^D. We, therefore, looked for soluble, disaggregated PrP^D by centrifuging both total PrP^D and the protease-resistant core of PrP^D from both strains following exposure to different combinations of Hsp90, Grp78, DnaJC1, and Stip1 at different pHs. The amount of PrP^D in pellets and supernatants was then compared by immunoblot (Fig. S4). In general, the majority of PrP^D was observed in the pellet samples and thus did not appear to be solubilized by the chaperones. Only ∼1% of the protease-resistant core of 22L PrP^D appeared to be solubilized and only in the presence of all chaperones at a pH of 5.5 (Fig. S4*B*, left panel). We re-analyzed the supernatants using longer gel exposure times to enhance the detection of soluble PrP^D at levels lower than 1% of total PrP^D (Fig. 9). Similar to what we observed previously in the absence of Hsp90 (Fig. 5), the protease-resistant core of 22L PrP^D was relatively more susceptible to disaggregation than either total PrP^D 22L or PrP^D from 87V (Fig. 9*A*). The presence of Hsp90 significantly improved 22L PrP^D solubilization but only in the presence of Grp78 (Fig. 9*B*). Thus, the presence of both Grp78 and Hsp90 can stimulate some disaggregation of the protease-resistant core of 22L PrP^D despite being unable to sensitize the same PrP^D population to proteases (Fig. 7*A*). This is reminiscent of other studies with other aggregate and chaperone systems (51) and suggests that sensitization of PrP^D to proteases and disaggregation of PrP^D are separate processes that can be driven independently by chaperones.

Discussion

Molecular chaperones that maintain cellular proteostasis by processing and removing non-native protein aggregates are

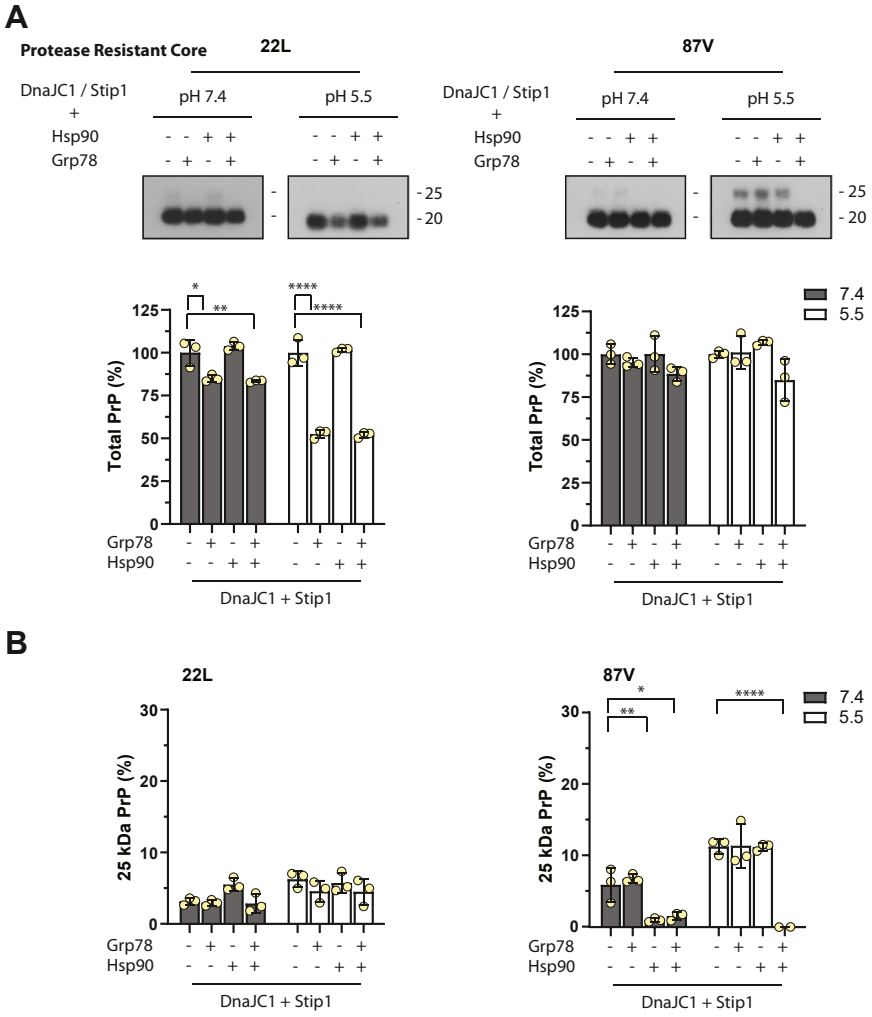

Figure 7. Hsp90 increases the exposure of full-length PrP^D in the protease-resistant core of PrP^D in a strain-specific manner. *A*, representative Western blots of the protease-resistant core of 22L (*upper left panels*) or 87V (*upper right panels*) PrP^D. PrP^D was mixed with DnaJC1 and Stip1 at a pH of 7.4 or 5.5 before being incubated with either Grp78, Hsp90, or Grp78/Hsp90, for 30 min in the presence of an ATP regeneration system. Samples were then treated with PK and de-glycosylated with PNGase F before being run over a gel and analyzed by Western blot with the 6D11 anti-PrP monoclonal antibody. Size markers indicating 25 kDa (*upper marker*) and 20 kDa (*lower marker*) are indicated to the *right* of each blot. The *lower panels* show the amount of 22L (*lower left*) and 87V (*lower right*) PrP^D remaining after PK treatment. *B*, the amount of 25 kDa, full-length, PrP^D remaining in the protease-resistant core of 22L (*left*) and 87V (*right*) PrP^D following exposure to chaperones and co-chaperones at pH 7.4 and 5.5. For all bar plots, data were calculated from n = 3 for each sample and are given as mean ± standard deviation. A one-way ANOVA with Tukey multiple comparisons within each pH data set was used to calculate the statistical significance. *Asterisks* represent a range of *p* values with p^* = 0.01 to 0.04, p^{**} = 0.005 to 0.009, and p^{****} = <0.0009. *Black bars* = pH 7.4; *white bars* = pH 5.5.

almost ubiquitous in cellular environments and modulating the concentration of chaperones *in vivo* influences the progression of prion disease (25, 52). In our previous studies, both 22L and 87V PrP^D were found to undergo changes in structure and protease-resistance during endocytosis (15, 19) and we considered that surface and endosome-associated chaperones like Grp78 and Hsp90 may contribute to the modification of PrP^D prior to degradation. In the current study, we characterized how environmental pH and protease pre-treatment affected the ability of an *in vitro* multi-chaperone system to influence the aggregation state and stability of PrP^D from two different prion strains, 22L and 87V. In general, chaperones disaggregated and sensitized 22L PrP^D to protease digestion better than 87V PrP^D, with chaperone activity enhanced by structural destabilization of PrP^D with a shift in pH from 7.4 to 5.5. While Grp78 alone was only able to sensitize 22L PrP^D to proteases, the co-chaperones Stip1 and DnaJC1 enabled Grp78 to also sensitize 87V PrP^D to proteases and facilitated destabilization of 22L PrP^D by Grp78. The addition of Hsp90 to the system promoted further structural changes in total PrP^D, but in a strain-specific manner. However, Hsp90 and co-chaperones provided little enhancement to the protease-sensitization activity of Grp78 against the protease-resistant core of PrP^D, which was also less sensitive to pH-induced destabilization. These data suggest that stability, and by correlation sensitivity to pH and chaperone-mediated destabilization, is heterogeneous across different populations of PrP^D.

Without Hsp90, Grp78 and its co-chaperones failed to significantly sensitize 22L total PrP^D to proteases at a pH of 7.4 in our assay. However, once it had been pre-treated with PK to yield its highly protease-resistant core, 22L PrP^D was actually more sensitive to disaggregation than total 22L PrP^D or any

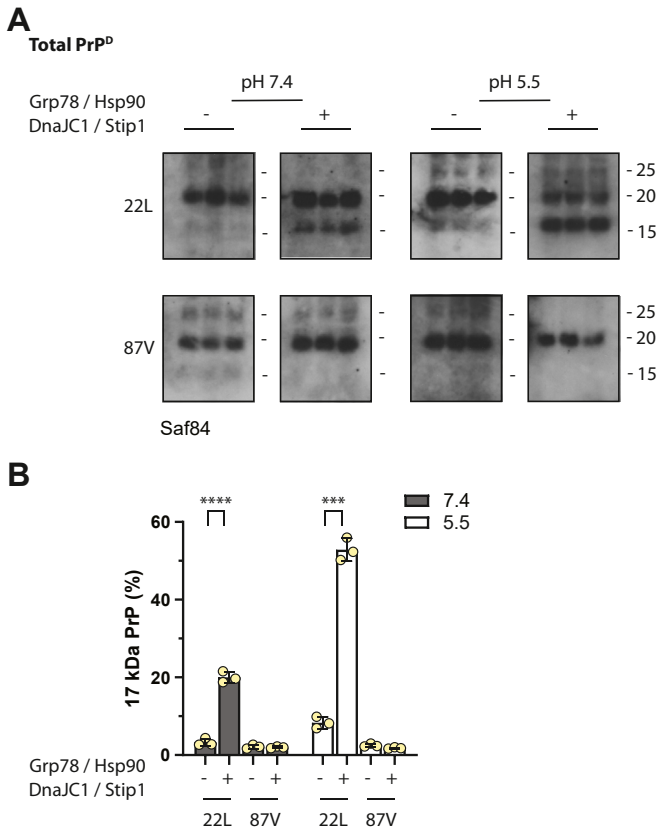

Figure 8. Increased protease-sensitivity of the n-terminus of PrP^D following interaction with chaperones is prion strain specific. *A*, immunoblots, developed with the anti-PrP monoclonal antibody Saf84 (epitope from a.a. 159–169), of 22L and 87V total PrP^D following exposure to chaperones and proteases at pH 7.4 and 5.5. All samples were digested with PK and de-glycosylated with PNGase F. Molecular mass markers for 25 kDa (*upper marker*), 20 kDa (*middle marker*), and 15 kDa (*lower marker*) are indicated to the *right* of each blot. *B*, quantification of the percentage of 16 kDa PrP^D relative to total PrP^D. Data were calculated from n = 3 for each sample and are given as mean ± standard deviation. A one-way ANOVA with a Tukey multiple comparisons test within each pH and strain data set was used to calculate the statistical significance. *Asterisks* represent *p*-values with $p^{***} = 0.0028$ and $p^{****} = <0.0009$. *Black bars* = pH 7.4; *white bars* = pH 5.5.

population of 87V PrP^D. These data strongly suggest that protease-sensitive portions of PrP^D have to be removed to enable either chaperone-mediated direct disaggregation or indirect disaggregation following structural destabilization. Our data are consistent with previous observations indicating that PrP^D aggregates are amalgamates of both protease-resistant and sensitive forms (15, 53–55), and suggest that either the protease-sensitive n-terminus of PrP^D or full-length, 25 kDa, protease-sensitive PrP^D may block chaperone access to protease-resistant regions of PrP^D. Alternatively, the presence of protease-sensitive PrP^D may enhance the overall stability of 22L aggregates. While the latter possibility is seemingly contradictory, structural heterogeneity has been documented to improve the resilience and durability of materials (56). Regardless of how the removal of protease-sensitive PrP^D influences the properties of prion aggregates, it is possible that timely clearance of PrP^D requires cycles of exposure to proteases to remove protease-sensitive material from the aggregate, thus exposing previously protected regions of PrP^D to chaperones.

In the absence of chaperones, the influence of low pH on 22L and 87V prions was heterogeneous across total PrP^D populations. The majority of both strains lost resistance to PK with acidification, while the protease-resistant PrP^D core of both strains underwent a change in structure that led to better protection of full-length, protease-sensitive PrP^D within the aggregate. This change in protection at low pH coincided with the appearance of a 23 kDa partial truncation product after PK treatment of either strain (Fig. 1*B*). A similar banding pattern was observed in 22L PrP^D taken up by cells (19) that was consistent with exposure of PrP^D to endosomal acidification during uptake and trafficking. However, a 23 kDa band was not observed in populations of 87V PrP^D after cellular uptake (19), despite the demonstration in this work of a similar sized band in 87V at low pH (Fig. 1*B*). Taken together, these data suggest that, in cells, either 87V PrP^D is not exposed to sufficiently low pH to lead to partial truncation of the n-terminus or cellular chaperones sensitize the n-terminus of 87V to proteases during uptake. This latter possibility is supported by our observation that the n-terminus of 87V PrP^D is greatly sensitized to proteases by Hsp90 and Stip1 (Fig. 7), which are also able to alter the conformation of PrP^C during the regulation of neuritogenesis (34, 38).

In previous studies, both 22L and 87V PrP^D were found to initially become more protease-sensitive shortly after cellular uptake, though cells began to accumulate highly protease-resistant and intermediate-sized aggregates over time (15). The initial drop in protease-resistance of PrP^D after cellular uptake was found to be dependent upon endosomal acidification. In light of our observations here, it is possible that low pH can both directly reduce the protease-resistance of PrP^D and promote the activity of chaperones by either destabilizing PrP^D before chaperone interaction or possibly by directly amplifying the activity of the chaperones. The intracellular accumulation of protease-resistant forms of 22L and 87V PrP^D over time could be the result of cells losing the ability to process PrP^D, possibly through exhaustion of the chaperone system, but could also result from cells slowly accumulating the populations of PrP^D most resistant to pH and chaperone-mediated structural destabilization. Thus, although our data show that changes in pH and chaperone activity can sensitize the majority of PrP^D to proteases relatively rapidly, the portions of PrP^D most recalcitrant to structural destabilization may take hours to clear in cellular environments, even under optimal circumstances.

In our chaperone assay, disaggregation by Grp78, Hsp90, and co-chaperones was improved when 22L PrP^D was pretreated with proteases, suggesting that disaggregation of PrP^D in cellular environments could require repeated cycles of exposure to chaperones and proteases for complete degradation. While we were unable to test time frames longer than 30 min due to limitations with the ATP regeneration system, it is also possible that disaggregation of total PrP^D could be observable over longer time frames, especially if it depends upon the initial unfolding of PrP^D around the n-terminal region of the prion protein. Previous work has found that lysosomal inhibition can reduce PrP^D accumulation (57),

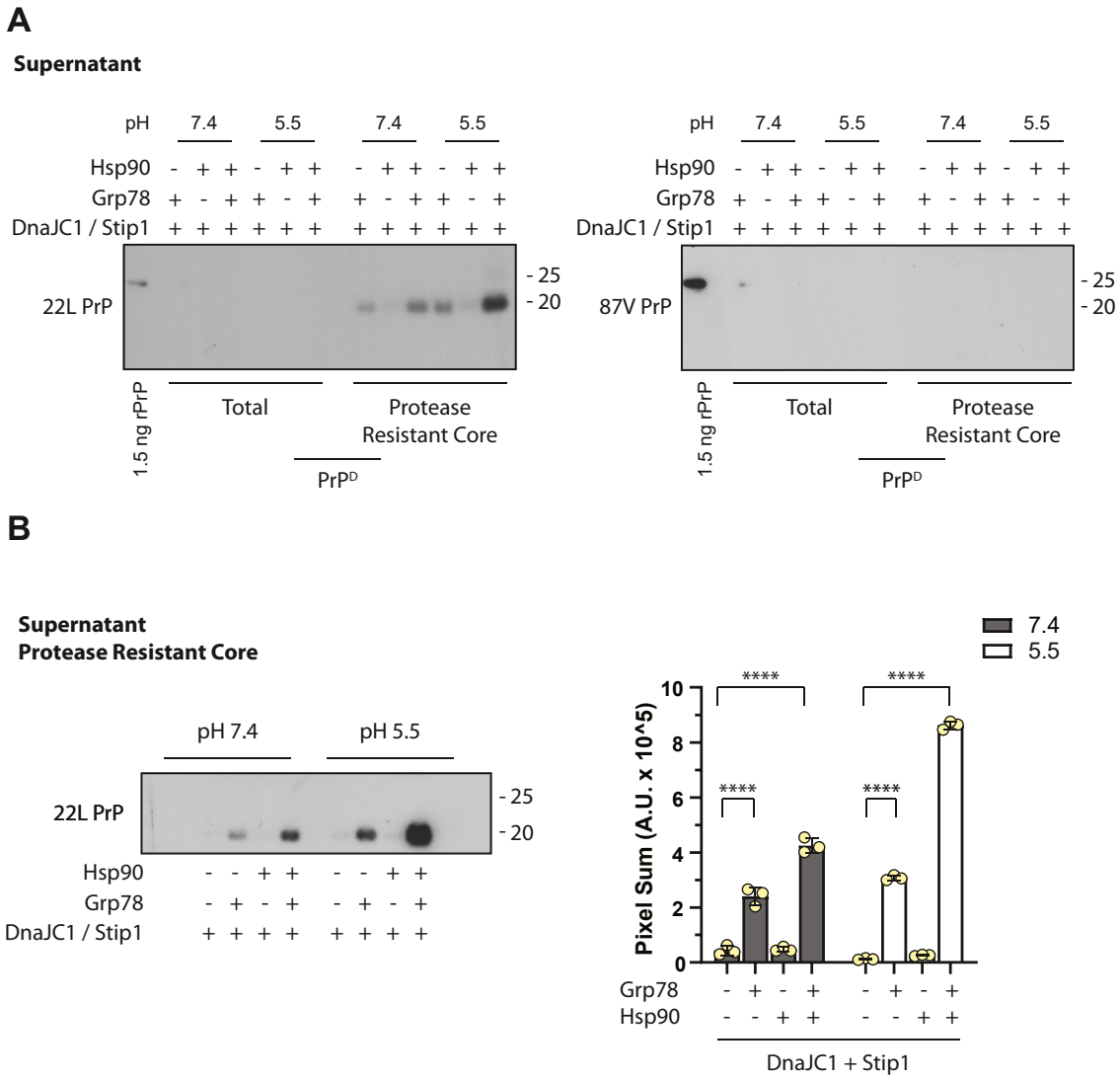

Figure 9. Hsp90 aids disaggregation of the protease-resistant core of 22L PrP^D by Grp78, DnaJC1, and Stip1. *A*, representative Western blots of disaggregated, soluble total PrP^D and the protease-resistant core of 22L (*left panel*) and 87V (*right panel*) PrP^D following incubation with DnaJC1 and Stip1 in the presence of Hsp90, Grp78, or Grp78/Hsp90, at pH 7.4 and 5.5 for 30 min. Blots were developed with the anti-PrP antibody 6D11. Samples were run alongside 1.5 ng of recombinant PrP (rPrP) to control for exposure between both blots. *B*, a representative long-exposure immunoblot showing the amount of the protease-resistant core of 22L PrP^D disaggregated following incubation with DnaJC1 and Stip1 in conjunction with Hsp90, Grp78, or Grp78/Hsp90 (*left panel*). Samples are the same supernatant samples shown in Fig. S4. All samples were PNGase F treated. Molecular mass markers for 25 kDa (*upper marker*) and 20 kDa (*lower marker*) are shown to the *right* of each blot. Quantification of the data is shown in the bar graph in the *right panel*. The amount of PrP^D is given as a pixel sum in arbitrary units. Data shown were calculated from n = 3 for each sample and are given as mean ± standard deviation. A one-way ANOVA with a Tukey multiple comparisons test within each pH data set was used to calculate the statistical significance. $p^{****} = <0.0009$.

indicating that lysosomal activity may, paradoxically, contribute to prion conversion. Thus, it is possible that clearance of less recalcitrant layers of PrP^D aggregates may expose sites of prion conversion on the protease-resistant core of PrP^D leading to new PrP^D formation that may negate PrP^D degradation. Alternatively, structural or conformational modification during trafficking to the lysosome may facilitate PrP^C conversion after PrP^D cycles out of the lysosome. Thus, the chaperones and proteases responsible for clearing PrP^D may actually promote prion conversion by acting as a 'proof-reading' system for prion conversion that clears away less stable forms of PrP^D prior to the next round of prion conversion. Regardless of whether chaperones ultimately interfere with or inadvertently contribute to prion propagation, this work demonstrates that chaperones can contribute to prion processing and may be targeted for therapeutic intervention during prion infection, perhaps by stimulating interactions between different chaperones to maximize their ability to interact with and degrade prion aggregates.

Experimental procedures

Animal care and propagation of prions

C57BL/10 and VMDK mice were used to respectively propagate 22L and 87V as described previously (16). Mice were euthanized after becoming clinically positive for prion disease and brains were harvested and stored at −80 °C until use. Protocols for inoculation, care to onset of prion disease,

and euthanasia in the *Guide for the Care and Use of Laboratory Animals* of the National Institutes of Health were rigorously followed for all mice used to propagate prions. The Rocky Mountain Laboratories Animal Care and Use Committee reviewed and approved the protocol used for animal experiments (protocol number 2021-023-E).

Preparation of PrP^D brain homogenate and phosphotungstate acid (PTA) precipitation

As described previously (15), brains harvested from 22L and 87V infected mice were homogenized with a Mini-BeadBeater-8 instrument (Biospec) in phosphate-buffered saline to a concentration of 10% (wt/vol). For each strain, brain homogenate stocks were composed of ten brains from clinically positive mice. Samples were clarified *via* centrifugation at 500*g* for 5 min after homogenization. Clarified brain homogenates were mixed 1:1 with 4% sarkosyl, vortexed, and incubated for 30 min at 37 °C. The 2% sarkosyl and brain homogenate solutions were then mixed with benzonase (Sigma) and magnesium chloride to a final concentration of 0.05 Units/μl and 1 mM, respectively. After a brief vortex, brain homogenate samples were incubated for 45 min at 37 °C. Benozonase treated brain homogenates were then centrifuged at 5000*g* for 5 min and supernatants were removed and split into two samples. One sample was treated with 50 μg/ml proteinase K (PK; Novagen) for 1 h at 37 °C while the second sample was not. Throughout this work we will refer to PrP^D that was treated with PK prior to sodium phosphotungstate acid hydrate (PTA; Sigma) precipitation as the protease-resistant core of PrP^D and material that was not pre-treated with PK during PTA precipitation as total PrP^D.

Both PK-treated and untreated brain homogenates were then mixed with Pefabloc (Sigma) and PTA to a final concentration of 5 mM and 3.2 μg/ml, respectively, before being incubated for 1.5 h at 37 °C. PrP^D was then pelleted with a 16,000*g* centrifugation for 30 min at room temperature. Pellets were washed in PBS containing 0.1 M EDTA and vortexed before being incubated at 37 °C for 30 min. PrP^D was again pelleted with a 16,000*g* centrifugation for 30 min at room temperature. Pellets were then resuspended in PBS before being mixed with glycerol to 15%, snap frozen, and stored at −80 °C until use. Sample replicates in each assay were derived from a single sample aliquot.

Plasmids, protein expression, and protein purification

Purification for Grp78, Stip1, and DnaJC1 was carried out similarly to, but modified from, previous work (27, 58). The Grp78, Stip1, and DnJC1 proteins were expressed in and purified from a bacterial expression system while the Hsp90 protein was purified directly from mouse brain. The genes for Grp78, Stip1, and DnaJC1 were engineered by Genescript into the pET-14b plasmid behind a cleavable affinity tag. The affinity tag for Grp78 and Stip1 was a cleavable His6x Sumo protein tag and the affinity tag used for DnaJC1 was a His6x tag with a thrombin cleavage site. While the genes for Grp78 and Stip1 were unmodified wild-type genes from mice, the gene for DnaJC1 was modified to only code for the luminal domain of the protein, amino acids 46 to 148. This region of DnaJC1 completely encompasses the J-domain of the protein and was previously found to be both properly folded and to stimulate the ATPase activity of both Grp78 and the bacterial Hsp70 DnaK (27). Throughout the article, this truncated form of DnaJC1 will be referred to as DnaJC1.

E. coli BL21(DE3) competent cells (ThermoFisher) were transformed by heat shock at 42 °C with the pET-14b plasmids containing the genes for Grp78, Stip1, and DnaJC1. Colonies of *E. coli* containing the pET-14b plasmid were identified *via* antibiotic selection and were grown up at 37 °C while being shaken at 200 rpm to an OD_{600} of 0.6 before expression of each gene was induced with isopropyl-1-thio-β-D-galactopyranoside (Sigma) at a final concentration of 0.4 mM. Both Grp78 and DnaJC1 were induced at 37 °C for 3 to 4 h while Stip1 was induced at 18 °C for 24 to 36 h. After induction, the bacteria were pelleted with a 5000*g* spin at 4 °C and pellets were stored at −80 °C until proteins could be purified. Pelleted *E. coli* containing Grp78, Stip1, and DnaJC1 were thawed on ice and resuspended in a phosphate lysis buffer (50 mM NaH_2PO_4 pH 8.0, 300 mM NaCl, 10 mM imidazole, 5 mM β-mercaptoethanol, 10% sucrose) containing 2× cOmplete Mini EDTA-free protease inhibitor cocktail (Sigma). Resuspended cells were then lysed by three passages through a French press cell disrupter (ThermoFisher). Cell lysates were clarified *via* centrifugation at 35,000*g* for 30 min.

All bacterial lysates containing Grp78, Stip1, and DnaJC1 were initially run over an Ni-NTA Superflow resin (Qiagen), and proteins that bound non-specifically to the resin were washed away in a phosphate-based wash buffer (25 mM NaH_2PO_4 pH 8.0, 300 mM NaCl, 20 mM imidazole, 5 mM β-mercaptoethanol). Grp78, Stip1, and DnaJC1 were eluted from the Ni-NTA column with a series of elution steps in wash buffer containing 25, 50, 100, 200, and 400 mM imidazole. Elution fractions for each protein that were determined by SDS-PAGE to have the highest concentration and purity were pooled and dialyzed against wash buffer overnight with either 5 units of SUMO protease (ThermoFisher) for Grp78 and Stip1 or 2.5 units of thrombin (ThermoFisher) for DnaJC1 to remove affinity tags. Once cleavage of affinity tags was >95% complete, Grp78, Stip1, and DnaJC1 were run over back over a Ni-NTA Superflow resin. The flow through was kept and protein was buffer exchanged into an ion exchange column loading buffer (50 mM Tris-HCl pH 7.4, 25 mM NaCl, 0.1 mM EDTA, 5 mM β-mercaptoethanol) by dialysis. Dialyzed Grp78, Stip1, and DnaJC1 were then run over a HiTrap Q HP column (Cytivia) and eluted over a long linear gradient from 25 to 1000 mM NaCl generated from ion exchange column loading buffer and elution buffer (50 mM Tris-HCl pH 7.4, 1000 mM NaCl, 0.1 mM EDTA, 5 mM β-mercaptoethanol). The purest fractions, determined *via* SDS-PAGE, were pooled and then both concentrated and buffer exchanged *via* Amicon Ultra spin concentrators (Millipore) into a storage buffer (50 mM Tris-HCl pH 7.4, 150 mM KCl, 0.05 mM EDTA, 15% glycerol, 2 mM dithiothreitol) before being snap frozen and stored at −80 °C until use. While the purity of Grp78, Stip1, and

DnaJC1 was typically greater than 99% after elution from the Q column, in cases where a significant amount of a contaminating protein was present proteins were either rerun over the Q column or cleaned with a run-over a superdex size exclusion column (Cytivia) equilibrated and run with 50 mM Tris-HCl pH 7.4, 150 mM KCl, 0.05 mM EDTA, and 2 mM dithiothreitol.

Purification of Hsp90 was modified from, but performed similarly to, previous work (59). For purification of Hsp90, brains from prion protein gene (*Prnp*) knockout mice (60) were homogenized with a Mini-BeadBeater-8 (BioSpec Products) to a final 10% w/v brain homogenate in a Tris lysis buffer (50 mM Tris-HCl pH 7.4, 100 mM NaCl, 5 mM β-mercaptoethanol, 10% sucrose) containing 2× cOmplete Mini protease inhibitor cocktail. Brain homogenates were initially clarified with a 500*g* spin for 5 min before being transferred to a new tube and clarified further with a 35,000*g* spin for 30 min. Clarified homogenates of *Prnp* knockout mouse brains, prepared at 10% w/v in 1× PBS, were diluted to 0.1% brain homogenate in ion exchange column load buffer before being loaded onto a HiTrap DEAE Sepharose FF column (Cytivia). Hsp90 was eluted from the DEAE column with a long linear gradient from 25 to 1000 mM NaCl generated from ion exchange column loading buffer and elution buffer. SDS-PAGE gel was used to determine the fractions with the highest purity of Hsp90, which were then pooled and buffer exchanged *via* Amicon Ultra spin concentrator into ion exchange column loading buffer before being loaded onto a HiTrap Heparin HP column (Cytivia). Hsp90 was eluted from the heparin column similarly to the DEAE column with a long linear gradient from 25 to 1000 mM NaCl generated from ion exchange column loading buffer and elution buffer. SDS-PAGE gel analysis was again used to determine the fractions with the highest purity of Hsp90. The highest purity fractions were pooled and diluted 1:10 into ion exchange column loading buffer containing KCl as opposed to NaCl before being loaded onto a HiTrap Q HP column. Hsp90 was eluted with a long linear gradient from 25 to 750 mM KCl generated from ion exchange column loading buffer and elution buffer that both contained KCl as opposed to NaCl. Fractions containing the highest purity of Hsp90 by SDS-PAGE were pooled and concentrated by dialysis against concentration buffer (50 mM Tris-HCl pH 7.4, 150 mM KCl, 0.05 mM EDTA, 20% dextran, 2 mM dithiothreitol). After concentration, Hsp90 was then mixed with 2× storage buffer, snap frozen, and stored at −80 °C. Samples of Hsp90 were >95% pure at the end of purification and were determined *via* mass spectrometry to contain 80 and 20% alpha and beta forms of Hsp90 respectively. The activity of the purified chaperones was verified with a luciferase refolding assay prepared similarly to previous studies (21, 58) (Fig. S5).

PrP^D pH-dependent protease-resistance assay

Stock solutions of 22L and 87V PrP^D that were PTA precipitated with and without PK treatment were diluted into disaggregation buffer (50 mM HEPES, 150 mM KOAc, 10 mM $MgOAc_2$, and 2 mM DTT) with pH values of 7.4, 7.0, 6.5, 6.0, and 5.5. PrP^D solutions were allowed to sit for 15 min at room temperature before being mixed with PK to a concentration of 10 μg/ml and incubated at 37 °C for 1 h. The pH range where PK has the highest activity is 8 to 9 and activity decreases with pH. However, PK is stable and functional down to a pH range of 4 to 5 (61, 62). After digestion, all samples were mixed with Pefabloc to 5 mM and were incubated at room temperature for 10 min to stop the activity of PK.

Assay for chaperone-mediated changes in PrP^D

Different combinations of Grp78, Hsp90, DnaJC1, and Stip1 were mixed with 22L and 87V PrP^D that had, or had not, been treated with PK before PTA precipitation. The concentration of 22L and 87V PrP^D was then determined *via* Western blot and PrP^D samples were diluted to the same concentration for each assay. All reactions were carried out in pH 7.4 or 5.5 disaggregation buffer and all reaction solutions contained 0.1 μM of PrP^D, 2 mM ATP (Sigma), and an ATP regeneration system composed of 0.25 μM creatine kinase (Sigma) and 2 mM creatine phosphate (Sigma). Creatine kinase has been used in previous studies to replenish ATP in chaperone assays (51) as the rate at which creatine kinase regenerates ATP is much faster than the rate at which chaperones can deplete it. While the activity of creatine kinase varies between pH 7.4 and 5.5 (63), the rate of ATP hydrolysis by Grp78 and Hsp90 is still much lower than the rate at which creatine kinase converts ADP to ATP. In all reactions with Grp78 and Hsp90, their concentrations were 2 μM and 1 μM respectively. In experiments where DnaJC1 and Stip1 were mixed together their concentrations were 0.5 μM. However, when they were tested individually, their concentrations were 1 μM. Chaperone reactions were carried out at 37 °C for 30 min in an Eppendorf Thermo Mixer C with shaking at 300 rpm. After 30 min, reaction samples were diluted 1:1 with a disaggregation buffer of the same pH as the reaction buffer before samples were split into two equal volumes to test for protease-resistance and disaggregation of PrP^D.

To test for changes in protease-resistance after chaperone interaction, half of each reaction mixture was mixed with PK to a final concentration of 10 μg/ml before being incubated at 37 °C for 1 h. Samples were treated with 5 mM Pefabloc at room temperature for 10 min to inhibit the activity of PK. The other half of each reaction was used to test for disaggregation by separating small solubilized PrP^D aggregates and monomers from large insoluble aggregates *via* centrifugation-induced sedimentation of larger PrP^D aggregates. Sedimentation was performed by centrifuging reaction samples over a layer of 10% sucrose at 18,300*g* in an F301.5 Beckmann rotor at 4 °C for 30 min. Supernatants were removed and pellets were resuspended in 2× NuPAGE sample buffer. As a size standard, a mixture of 15 to 600 kDa protein standards (Sigma) was run over a 0 to 20% sucrose gradient in order to approximate the size of PrP^D in the supernatant and pellet samples. No protein in the 15 to 600 kDa mixture was detected beyond fraction 5, which roughly correlates to 10% sucrose (Fig. S6).

SDS-PAGE and Western blots

PK treated samples of 22L and 87V PrP^D were mixed with 4× NuPage sample buffer (Novex) to a final concentration of 1.5× before being heat denatured at 95 °C for 5 min. De-glycosylation of indicated samples was performed with PNGase F (NEB) by first mixing 12 µl of sample in NuPAGE sample buffer with 1 µl of glycoprotein denaturing buffer (NEB). Samples were then denatured by heating at 95 °C for 5 min before being mixed with 1 µl each of glycobuffer (NEB), NP-40 (NEB), and PNGase F (500,000 U/ml) and incubated at 37 °C overnight. De-glycosylated samples were heated to 95 °C for 5 min again prior to being run on gels. Gels were run for ∼3 h, or until the dye front reached the bottom of the gel, at a constant voltage of 75 V. Proteins in each gel were transferred to polyvinylidene difluoride (PVDF, EMD Milipore) Immobilon-P membranes with a NuPAGE Novex gel system run at a constant 34 V overnight.

PVDF membranes were blocked with a 5% powdered milk and TBST solution, (10 mM Tris HCl (pH 8.0), 150 mM NaCl, 0.05% Tween 20, 5% powdered milk (wt/vol)), for 1 h at room temperature. Blots were then probed with either the anti-PrP antibody 6D11 (BioLegends, antibody epitope to PrP^C residues 93–109) or Saf84 (Cayman Chemical Co, antibody epitope to PrP^C residues 159–169) that were both diluted to 1:10,000 in TBST. After a 1.5 h incubation, membranes were rinsed four times with TBST over 30 min. Membranes were then incubated with a sheep anti-mouse secondary antibody conjugated to horseradish peroxidase (GE Amersham) at a 1:40,000 dilution for 1 h before membranes were rinsed four times with TBST over 30 min. Blots were developed with the ECL Plus reagent (GE Healthcare Life Sciences) and developed on photosensitive film. Digital scans of the developed film were processed using Un-Scan-IT software (version 7.1; Silk Scientific Corporation).

Quantification of blots, data analysis, and calculations

Bands of PrP were quantified from scans of film similarly to previous work (15) using the "Segment Analysis" tool in the Un-Scan-IT software. Bands of PrP in each lane were quantified *via* summation of all pixels in user-defined "boxes" or analysis regions. Quantified PrP bands were background corrected by subtraction of an average background value calculated by taking the average of four boxes near each PrP band. Data not represented as a pixel sum value was divided by the average pixel sum of a piece of data within the same data set, which was then multiplied by 100 in order to normalize all data in a set to a percentage of one piece of data in the set.

For the line graphs in Figures 1 and 3, all of the data for each line was processed by dividing the pixel sum for each pH by the average pixel sum of data from pH 7.4 in order to show how protease-resistance changes with a drop from pH 7.4 to 5.5. Data in bar plots showing the change in 22L and 87V PrP^D populations after chaperone exposure were prepared by dividing all data in a set by the average pixel sum of control data containing either no chaperones (Figs. 1 and 3) or a combination of the co-chaperones DnaJC1 and Stip1 (Figs. 2, 4, 6 and 7). For PNGase F treated samples, percentages of full-length, 25 kDa PrP^D, or partially truncated 16 kDa PrP^D, were calculated by dividing the pixel sum of the 25 or 16 kDa PrP^D bands by the total amount of PrP^D in each lane and then multiplying by 100. All bands were background corrected before ratio calculations. In all plots, data are shown as an average of three sample replicates with error bars representing the standard deviation. Statistical analysis for each data set was done in Prism Graphpad Software (version 8.0.2). In figures, the asterisks represent *p*-values for CI = 95% within specific ranges with p^* = 0.01 to 0.04, p^{**} = 0.005 to 0.009, p^{***} = 0.001 to 0.004, and p^{****} = <0.0009.

Data analysis

All values are expressed as the mean ± SD from n = 3 samples for data shown in main text figures and n = 4 for Figure S1. The significance of line plots in Figures 1 and 2 were calculated via two-way ANOVA using a Tukey's multiple comparison. For the Bar plots in Figures 1–5, where only two samples were compared at time, significance was calculated via unpaired one-tailed *t* tests while significance tests of data in bar plots comparing multiple samples, such as those in Figures 6–9 and Figure S1, were performed with one-way ANOVA using a Tukey's multiple comparison.

Data availability

Data are shared upon request.

Supporting information—This article contains supporting information.

Acknowledgment—We thank Dr Simote Foliaki, Dr Cathryn Haigh, and Dr James Carroll for insightful discussion and commentary on the manuscript and Dr Yixiang Zhang for assistance with mass spectrometry.

Author contributions—D. S. and S. A. P. conceptualization; D. S. methodology; D. S. validation; D. S. formal analysis; D. S. investigation; D. S. resources; D. S. data curation; D. S. writing–original draft; D. S. and S. A. P. writing–review & editing; D. S. visualization; S. A. P. supervision; S. A. P. project administration; S. A. P. funding acquisition.

Funding and additional information—This research was supported by a grant from the National Institutes of Health, National Institute of Allergy and Infectious Diseases, Division of Intramural Research. The content is solely the responsibility of the authors and does not necessarily represent the official views of the National Institutes of Health.

Conflict of interest—The authors declare that they have no known competing financial interests or personal relationships that could have appeared to influence the work reported in this paper.

Abbreviations—The abbreviations used are: ER, endoplasmic reticulum; PK, proteinase K; PrP^C, protease-sensitive mammalian prion

protein; PrP^D, disease-associated prion protein aggregates; PVDF, polyvinylidene difluoride.

References

1. Colby, D. W., and Prusiner, S. B. (2011) Prions. *Cold Spring Harb. Perspect. Biol.* **3**, a006833
2. Gill, A. C., and Castle, A. R. (2018) The cellular and pathologic prion protein. *Handb. Clin. Neurol.* **153**, 21–44
3. Goold, R., Rabbanian, S., Sutton, L., Andre, R., Arora, P., Moonga, J., *et al.* (2011) Rapid cell-surface prion protein conversion revealed using a novel cell system. *Nat. Commun.* **2**, 281
4. Yim, Y. I., Park, B. C., Yadavalli, R., Zhao, X., Eisenberg, E., and Greene, L. E. (2015) The multivesicular body is the major internal site of prion conversion. *J. Cell Sci.* **128**, 1434–1443
5. Arnold, J. E., Tipler, C., Laszlo, L., Hope, J., Landon, M., and Mayer, R. J. (1995) The abnormal isoform of the prion protein accumulates in late-endosome-like organelles in scrapie-infected mouse brain. *J. Pathol.* **176**, 403–411
6. Caughey, B., and Raymond, G. J. (1991) The scrapie-associated form of PrP is made from a cell surface precursor that is both protease- and phospholipase-sensitive. *J. Biol. Chem.* **266**, 18217–18223
7. Hoyt, F., Alam, P., Artikis, E., Schwartz, C. L., Hughson, A. G., Race, B., *et al.* (2022) Cryo-EM of prion strains from the same genotype of host identifies conformational determinants. *PLoS Pathog.* **18**, e1010947
8. Caughey, B., Raymond, G. J., and Bessen, R. A. (1998) Strain-dependent differences in β-sheet conformations of abnormal prion protein. *J. Biol. Chem.* **273**, 32230–32235
9. Bessen, R. A., Kocisko, D. A., Raymond, G. J., Nandan, S., Lansbury, P. T., and Caughey, B. (1995) Non-genetic propagation of strain-specific properties of scrapie prion protein. *Nature* **375**, 698–700
10. Legname, G., Nguyen, H.-O. B., Peretz, D., Cohen, F. E., DeArmond, S. J., and Prusiner, S. B. (2006) Continuum of prion protein structures enciphers a multitude of prion isolate-specified phenotypes. *Proc. Natl. Acad. Sci. U. S. A.* **103**, 19105–19110
11. Bessen, R. A., and Marsh, R. F. (1992) Identification of two biologically distinct strains of transmissible mink encephalopathy in hamsters. *J. Gen. Virol.* **73**, 329–334
12. Morales, R., Abid, K., and Soto, C. (2007) The prion strain phenomenon: molecular basis and unprecedented features. *Biochim. Biophys. Acta Mol. Basis Dis.* **1772**, 681–691
13. Bett, C., Joshi-Barr, S., Lucero, M., Trejo, M., Liberski, P., Kelly, J. W., *et al.* (2012) Biochemical properties of highly neuroinvasive prion strains. *PLoS Pathog.* **8**, e1002522
14. Fehlinger, A., Wolf, H., Hossinger, A., Duernberger, Y., Pleschka, C., Riemschoss, K., *et al.* (2017) Prion strains depend on different endocytic routes for productive infection. *Sci. Rep.* **7**, 6923
15. Shoup, D., and Priola, S. A. (2021) The size and stability of infectious prion aggregates fluctuate dynamically during cellular uptake and disaggregation. *Biochemistry* **60**, 398–411
16. Choi, Y. P., and Priola, S. A. (2013) A specific population of abnormal prion protein aggregates is preferentially taken up by cells and disaggregated in a strain-dependent manner. *J. Virol.* **87**, 11552–11561
17. Goold, R., McKinnon, C., Rabbanian, S., Collinge, J., Schiavo, G., and Tabrizi, S. J. (2013) Alternative fates of newly formed PrPSc upon prion conversion on the plasma membrane. *J. Cell Sci.* **126**, 3552–3562
18. Caughey, B., Raymond, G. J., Ernst, D., and Race, R. (1991) N-terminal truncation of the scrapie-associated form of PrP by lysosomal protease (s): implications regarding the site of conversion of PrP to the protease-resistant state. *J. Virol.* **65**, 6597–6603
19. Shoup, D., and Priola, S. A. (2023) Full-length prion protein incorporated into prion aggregates is a marker for prion strain-specific destabilization of aggregate structure following cellular uptake. *J. Biochem.* **174**, 165–181
20. Chen, W., van der Kamp, M. W., and Daggett, V. (2014) Structural and dynamic properties of the human prion protein. *Biophys. J.* **106**, 1152–1163
21. Shorter, J. (2011) The mammalian disaggregase machinery: Hsp110 synergizes with Hsp70 and Hsp40 to catalyze protein disaggregation and reactivation in a cell-free system. *PLoS One* **6**, e26319
22. Tiwari, S., Fauvet, B., Assenza, S., De Los Rios, P., and Goloubinoff, P. (2023) A fluorescent multi-domain protein reveals the unfolding mechanism of Hsp70. *Nat. Chem. Biol.* **19**, 198–205
23. Lin, Z., Puchalla, J., Shoup, D., and Rye, H. S. (2013) Repetitive protein unfolding by the trans ring of the GroEL-GroES chaperonin complex stimulates folding. *J. Biol. Chem.* **288**, 30944–30955
24. Rosenzweig, R., Nillegoda, N. B., Mayer, M. P., and Bukau, B. (2019) The Hsp70 chaperone network. *Nat. Rev. Mol. Cell Biol.* **20**, 665–680
25. Park, K. W., Eun Kim, G., Morales, R., Moda, F., Moreno-Gonzalez, I., Concha-Marambio, L., *et al.* (2017) The endoplasmic reticulum chaperone GRP78/BiP modulates prion propagation in vitro and in vivo. *Sci. Rep.* **7**, 44723
26. Misra, U. K., Gonzalez-Gronow, M., Gawdi, G., and Pizzo, S. V. (2005) The role of MTJ-1 in cell surface translocation of GRP78, a receptor for alpha 2-macroglobulin-dependent signaling. *J. Immunol.* **174**, 2092–2097
27. Chevalier, M., Rhee, H., Elguindi, E. C., and Blond, S. Y. (2000) Interaction of murine BiP/GRP78 with the DnaJ homologue MTJ1. *J. Biol. Chem.* **275**, 19620–19627
28. Vorberg, I., Raines, A., and Priola, S. A. (2004) Acute formation of protease-resistant prion protein does not always lead to persistent scrapie infection in vitro. *J. Biol. Chem.* **279**, 29218–29225
29. Merkel, A., Chen, Y., and George, A. (2019) Endocytic trafficking of DMP1 and GRP78 complex facilitates osteogenic differentiation of human periodontal ligament stem cells. *Front. Physiol.* **10**, 1175
30. Tamayo, A. G., Slater, L., Taylor-Parker, J., Bharti, A., Harrison, R., Hung, D. T., *et al.* (2011) GRP78(BiP) facilitates the cytosolic delivery of anthrax lethal factor (LF) in vivo and functions as an unfoldase in vitro. *Mol. Microbiol.* **81**, 1390–1401
31. Wallabregue, A., Moreau, D., Sherin, P., Moneva Lorente, P., Jarolímová, Z., Bakker, E., *et al.* (2016) Selective imaging of late endosomes with a pH-sensitive diazaoxatriangulene fluorescent probe. *J. Am. Chem. Soc.* **138**, 1752–1755
32. Lott, A., Oroz, J., and Zweckstetter, M. (2020) Molecular basis of the interaction of Hsp90 with its co-chaperone hop. *Protein Sci.* **29**, 2422–2432
33. Lopes, M. H., Hajj, G. N., Muras, A. G., Mancini, G. L., Castro, R. M., Ribeiro, K. C., *et al.* (2005) Interaction of cellular prion and stress-inducible protein 1 promotes neuritogenesis and neuroprotection by distinct signaling pathways. *J. Neurosci.* **25**, 11330–11339
34. Romano, S. A., Cordeiro, Y., Lima, L. M., Lopes, M. H., Silva, J. L., Foguel, D., *et al.* (2009) Reciprocal remodeling upon binding of the prion protein to its signaling partner hop/STI1. *FASEB J.* **23**, 4308–4316
35. Bhattacharya, K., and Picard, D. (2021) The Hsp70-Hsp90 go-between Hop/Stip1/Sti1 is a proteostatic switch and may be a drug target in cancer and neurodegeneration. *Cell. Mol. Life Sci.* **78**, 7257–7273
36. Hoyt, F., Standke, H. G., Artikis, E., Schwartz, C. L., Hansen, B., Li, K., *et al.* (2022) Cryo-EM structure of anchorless RML prion reveals variations in shared motifs between distinct strains. *Nat. Commun.* **13**, 4005
37. Liang, J., and Kong, Q. (2012) α-Cleavage of cellular prion protein. *Prion* **6**, 453–460
38. Maciejewski, A., Ostapchenko, V. G., Beraldo, F. H., Prado, V. F., Prado, M. A., and Choy, W.-Y. (2016) Domains of STIP1 responsible for regulating PrPC-dependent amyloid-β oligomer toxicity. *Biochem. J.* **473**, 2119–2130
39. Caetano, F. A., Lopes, M. H., Hajj, G. N., Machado, C. F., Pinto Arantes, C., Magalhães, A. C., *et al.* (2008) Endocytosis of prion protein is required for ERK1/2 signaling induced by stress-inducible protein 1. *J. Neurosci.* **28**, 6691–6702
40. Krukenberg, K. A., Southworth, D. R., Street, T. O., and Agard, D. A. (2009) pH-dependent conformational changes in bacterial Hsp90 reveal a Grp94-like conformation at pH 6 that is highly active in suppression of citrate synthase aggregation. *J. Mol. Biol.* **390**, 278–291
41. Jin, Y., Hoxie, R. S., and Street, T. O. (2017) Molecular mechanism of bacterial Hsp90 pH-dependent ATPase activity. *Protein Sci.* **26**, 1206–1213

42. Casey, J. R., Grinstein, S., and Orlowski, J. (2010) Sensors and regulators of intracellular pH. *Nat. Rev. Mol. Cell Biol.* **11**, 50–61
43. Hu, Y. B., Dammer, E. B., Ren, R. J., and Wang, G. (2015) The endosomal-lysosomal system: from acidification and cargo sorting to neurodegeneration. *Transl. Neurodegener.* **4**, 18
44. Colby, D. W., Giles, K., Legname, G., Wille, H., Baskakov, I. V., DeArmond, S. J., *et al.* (2009) Design and construction of diverse mammalian prion strains. *Proc. Natl. Acad. Sci. U. S. A.* **106**, 20417–20422
45. Saverioni, D., Notari, S., Capellari, S., Poggiolini, I., Giese, A., Kretzschmar, H. A., *et al.* (2013) Analyses of protease resistance and aggregation state of abnormal prion protein across the spectrum of human prions. *J. Biol. Chem.* **288**, 27972–27985
46. Wegele, H., Haslbeck, M., Reinstein, J., and Buchner, J. (2003) Sti1 is a novel activator of the Ssa proteins. *J. Biol. Chem.* **278**, 25970–25976
47. Song, Y., and Masison, D. C. (2005) Independent regulation of Hsp70 and Hsp90 chaperones by Hsp70/Hsp90-organizing protein Sti1 (Hop1). *J. Biol. Chem.* **280**, 34178–34185
48. Masison, D. C., Reidy, M., and Kumar, J. (2022) J proteins counteract amyloid propagation and toxicity in yeast. *Biology (Basel)* **11**, 1292
49. Kim, C. L., Umetani, A., Matsui, T., Ishiguro, N., Shinagawa, M., and Horiuchi, M. (2004) Antigenic characterization of an abnormal isoform of prion protein using a new diverse panel of monoclonal antibodies. *Virology* **320**, 40–51
50. Kocisko, D. A., Lansbury, P. T., and Caughey, B. (1996) Partial unfolding and refolding of scrapie-associated prion protein: evidence for a critical 16-kDa C-terminal domain. *Biochemistry* **35**, 13434–13442
51. Shoup, D., Roth, A., Puchalla, J., and Rye, H. S. (2022) The impact of hidden structure on aggregate disassembly by molecular chaperones. *Front. Mol. Biosci.* **9**, 915307
52. Thackray, A. M., Lam, B., McNulty, E. E., Nalls, A. V., Mathiason, C. K., Magadi, S. S., *et al.* (2022) Clearance of variant Creutzfeldt-Jakob disease prions in vivo by the Hsp70 disaggregase system. *Brain* **145**, 3236–3249
53. Choi, Y. P., Head, M. W., Ironside, J. W., and Priola, S. A. (2014) Uptake and degradation of protease-sensitive and -resistant forms of abnormal human prion protein aggregates by human astrocytes. *Am. J. Pathol.* **184**, 3299–3307
54. Safar, J., Wille, H., Itri, V., Groth, D., Serban, H., Torchia, M., *et al.* (1998) Eight prion strains have PrP(Sc) molecules with different conformations. *Nat. Med.* **4**, 1157–1165
55. Thackray, A. M., Hopkins, L., Klein, M. A., and Bujdoso, R. (2007) Mouse-adapted ovine scrapie prion strains are characterized by different conformers of PrPSc. *J. Virol.* **81**, 12119–12127
56. Cranford, S. W. (2013) Increasing silk fibre strength through heterogeneity of bundled fibrils. *J. R. Soc. Interf.* **10**, 20130148
57. Doh-Ura, K., Iwaki, T., and Caughey, B. (2000) Lysosomotropic agents and cysteine protease inhibitors inhibit scrapie-associated prion protein accumulation. *J. Virol.* **74**, 4894–4897
58. Morán Luengo, T., Kityk, R., Mayer, M. P., and Rüdiger, S. G. D. (2018) Hsp90 breaks the deadlock of the Hsp70 chaperone system. *Mol. Cell* **70**, 545–552.e9
59. Yonezawa, N., Nishida, E., Sakai, H., Koyasu, S., Matsuzaki, F., Iida, K., *et al.* (1988) Purification and characterization of the 90-kDa heat-shock protein from mammalian tissues. *Eur. J. Biochem.* **177**, 1–7
60. Striebel, J. F., Race, B., Pathmajeyan, M., Rangel, A., and Chesebro, B. (2013) Lack of influence of prion protein gene expression on kainate-induced seizures in mice: studies using congenic, coisogenic and transgenic strains. *Neuroscience* **238**, 11–18
61. Ren, Y., Luo, H., Huang, H., Hakulinen, N., Wang, Y., Wang, Y., *et al.* (2020) Improving the catalytic performance of Proteinase K from Parengyodontium album for use in feather degradation. *Int. J. Biol. Macromol.* **154**, 1586–1595
62. Farrell, R. E. (2009) *RNA Methodologies: Laboratory Guide for Isolation and Characterization*, Elsevier Science, London, UK
63. Goudemant, J. F., vander Elst, L., Dupont, B., Van Haverbeke, Y., and Muller, R. N. (1994) pH and temperature effects on kinetics of creatine kinase in aqueous solution and in isovolumic perfused heart. A 31P nuclear magnetization transfer study. *NMR Biomed.* **7**, 101–110